THE FASEB JOURNAL • RESEARCH • www.fasebj.org

STAU1 binds to IBDV genomic double-stranded RNA and promotes viral replication *via* attenuation of MDA5-dependent β interferon induction

Chengjin Ye,*[,1] Zhaoli Yu,*[,1] Yiwei Xiong,[†] Yu Wang,* Yina Ruan,* Yueping Guo,* Mianmian Chen,* Shilu Luan,* Enli Zhang,* and Hebin Liu*[,†,2]

*Department of Veterinary Medicine, College of Animal Science and Technology, Zhejiang A&F University, Hangzhou, China; and [†]Department of Biological Sciences, Xi'an Jiaotong–Liverpool University, Suzhou, China

ABSTRACT: Infectious bursal disease virus (IBDV) infection triggers the induction of type I IFN, which is mediated by melanoma differentiation-associated protein 5 recognition of the viral genomic double-stranded RNA (dsRNA). However, the mechanism of IBDV overcoming the type I IFN antiviral response remains poorly characterized. Here, we show that IBDV genomic dsRNA selectively binds to the host cellular RNA binding protein Staufen1 (STAU1) *in vitro* and *in vivo*. The viral dsRNA binding region was mapped to the N-terminal moiety of STAU1 (residues 1–468). Down-regulation of STAU1 impaired IBDV replication and enhanced IFN-β transcription in response to IBDV infection, while having little effect on the viral attachment to the host cells and cellular entry. Conversely, overexpression of STAU1 but not the IBDV dsRNA–binding deficient STAU1 mutant (469–702) led to a suppression of IBDV dsRNA–induced IFN-β promoter activity. Moreover, we found that the binding of STAU1 to IBDV dsRNA decreased the association of melanoma differentiation-associated protein 5 but not VP3 with the IBDV dsRNA *in vitro*. Finally, we showed that STAU1 and VP3 suppressed IFN-β gene transcription in response to IBDV infection in an additive manner. Collectively, these findings provide a novel insight into the evasive strategies used by IBDV to escape the host IFN antiviral response.—Ye, C., Yu, Z., Xiong, Y., Wang, Y., Ruan, Y., Guo, Y., Chen, M., Luan, S., Zhang, E., Liu, H. STAU1 binds to IBDV genomic double-stranded RNA and promotes viral replication *via* attenuation of MDA5-dependent β interferon induction. FASEB J. 33, 286–300 (2019). www.fasebj.org

KEY WORDS: RNA-binding protein · innate antiviral response · RIG-I–like receptors

Infectious bursal disease virus (IBDV), a nonenveloped virus of the family *Birnaviridae*, is the causative agent of infectious bursal disease, an acute and highly contagious disease of young chickens. IBDV mainly targets the immature B cells in the bursa of Fabricius of chickens, resulting in immunosuppression and an increased susceptibility to secondary infections in young chickens (1). The genome of IBDV is a bisegmented double-strand RNA (dsRNA) molecule comprising 2 segments, segment A (3.2 kb) and segment B (2.8 kb). The small genome segment B contains 1 open reading frame (ORF) that encodes VP1, the putative RNA-dependent RNA polymerase of IBDV (2), whereas the large genome segment A contains 2 overlapping ORFs, ORF1 and ORF2, which encode the viral nonstructural protein VP5 involved in viral egress (3, 4) and a precursor polyprotein (pVP2-VP4-VP3) (5, 6), respectively. VP4 is a serine protease that cleaves the polyprotein (pVP2-VP4-VP3) to form separate VP2, VP4, and VP3. The VP2 is the major viral structural protein and assembles into 260 trimmers to form a $T = 13$ icosahedral IBDV capsid (7, 8). VP1 is present in virions both as a free polypeptide VP1 and as a genome-linked protein (VPg) that covalently links to the 5′ ends of the genomic RNA segments. VP3 interacts both with VP1 and viral dsRNA to assemble into RNP complexes (9, 10) in which it significantly stimulates the VP1 RdRp activity (11). Furthermore, both VP1 and VP3 are required and sufficient for the translation initiation of IBDV uncapped genomic dsRNA (12).

The host reaction to virus infection results in the release of a broad array of cellular proteins such as cytokines,

ABBREVIATIONS: chIFN-β, chicken IFN-β; chMDA5, chicken melanoma differentiation-associated protein 5; chSTAU1, chicken STAU1; dsRNA, double-stranded RNA; EGFP, enhanced green fluorescent protein; eIF2α, eukaryotic initiation factor 2 alpha; GAPDH, glyceraldehyde-3-phosphate dehydrogenase; HCV, hepatitis C virus; hpi, hour postinfection; IBDV, infectious bursal disease virus; IP, immunoprecipitation; MAVS, mitochondrial antiviral-signaling protein; MDA5, melanoma differentiation-associated protein 5; ORF, open reading frame; PKR, protein kinase R; qRT-PCR, quantitative RT-PCR; PRR, pattern recognition receptor; RIG-I, retinoic acid–inducible gene I; SG, stress granule; shEGFP, shRNA against EGFP; shRNA, short hairpin RNA; STAU1, Staufen1

[1] These authors contributed equally to this work.

[2] Correspondence: Zhejiang A&F University, 666 Wusu St., Hangzhou, Zhejiang, 311300, China. E-mail: hb1liu@foxmail.com

doi: 10.1096/fj.201800062RR

This article includes supplemental data. Please visit *http://www.fasebj.org* to obtain this information.

0892-6638/19/0033-0286 © FASEB

which affect virus productive infection. IFN-β is one of the major cytokines rapidly triggered by many viruses in infected cells; it plays a critical role in innate antiviral response (*e.g.*, inhibiting viral replication and inducing an antiviral state in cells that inhibits the spread of infection) (13). IFN-β induction is mainly mediated by the RNA helicases retinoic acid–inducible gene I (RIG-I) and melanoma differentiation-associated protein 5 (MDA5), two major cytoplasmic pattern recognition receptors (PRRs) that selectively sense cytoplasmic nonself RNAs (14). MDA5 recognizes genomic long-duplex RNAs of dsRNA viruses or dsRNA replication intermediates of positive-strand viruses, whereas RIG-I detects the 5′ triphosphate group and the blunt end of short dsRNAs or single-stranded RNA hairpins (15, 16). This recognition activates the key adaptor mitochondrial antiviral signaling protein (MAVS) and subsequently the downstream signal cascades that lead to IFN expression (17). In chicken, homologs of mammalian RIG-I are absent (18), and chicken MDA5 (chMDA5) possesses the same structure and functionally compensates for the deficiency of RIG-I (19, 20). Interestingly, unlike other chicken viruses, IBDV did not induce or induced very low levels of IFN-β production early in the viral infection in an *in vivo* animal infection model (21). The viral proteins of IBDV, VP3, and VP4 were reported to be involved in the antagonistic process in the regulation of IFN-β production in the IBDV infection. VP4 mediates the inhibition of IFN-β *via* an interaction with the glucocorticoid-induced leucine zipper (22), and VP3 competes with MDA5 to bind the intracellular viral genomic dsRNA to block IFN-β induction (23). Protein kinase R (PKR) serves as a cytoplasmic PRR for viral RNA with a double-stranded structure. Upon activation by dsRNA, PKR inhibits protein translation through phosphorylation of its natural substrate, eukaryotic translation initiation factor 2 alpha (eIF2α) (24). PKR also plays a primary role in mediating IFN antiviral activities of virus-infected cells during the replicative cycle of many RNA viruses. IFN induces the activation of PKR, which in return amplifies IFN-β induction in a feedback mechanism (25). IBDV viral protein VP3 prevents the VP2-triggered PKR activation, which exacerbates apoptosis of cells infected with IBDV upon exposure to IFN (26, 27).

Staufen1 (STAU1), a member of the RNA-binding protein family, plays a central role in the regulation of mRNA transport, translational control, and decay (28). STAU1 contains dsRNA-binding domains that bind RNAs with double-stranded secondary structures (29). In addition to its conserved role as an RNA regulator, STAU1 is also implicated in the regulation of the life cycles of many RNA viruses. STAU1 is implicated in genomic RNA encapsidation of HIV (30, 31), the transportation of the RNA of hepatitis C virus (HCV) to the site of translation and replication (32), and multiplication of influenza viruses *via* interaction with the viral RNPs and NS1 (33, 34). STAU1, together with PKR, are recruited and localized to stress granules (SGs) (35). Despite the importance of STAU1 in regulation of the viral life cycles in virus-infected cells, however, it remains unknown whether STAU1 can interact and sense the genomic dsRNA of IBDV and whether this action contributes to the regulation of IBDV productive infection. Here, we show for the first time that chicken STAU1 (chSTAU1) binds to IBDV dsRNA *via* its N-terminal moiety (residues 1–468). The interaction of chSTAU1 and the viral dsRNA promotes the IBDV replication *via* suppression of the viral dsRNA-induced chicken IFN-β (chIFN-β) production. Furthermore, the presence of chSTAU1 binding to IBDV dsRNA dampens the chMDA5 but not VP3 interaction with IBDV dsRNA, resulting in reduced chIFN-β production in response to IBDV infection. Finally, we show that chSTAU1 acts additively with VP3 to suppress the chIFN-β promoter transcription activity. Together, this study suggests that the host cellular chSTAU1 is utilized by IBDV as one strategy to escape host antiviral IFN response.

MATERIALS AND METHODS

Cell lines, virus strains, and reagents

HEK293T (CRL-11268; ATCC, Manassas, VA, USA), the chicken fibroblast cell line DF-1 (CRL-12203; ATCC), and the HeLa cell (CCL-2; ATCC) were routinely maintained in DMEM (Thermo Fisher Scientific, Waltham, MA, USA) supplemented with 10% fetal bovine serum (Thermo Fisher Scientific). DF-1 cells stably expressing the short hairpin RNA (shRNA) against chMDA5 were previously described (23). IBDV-attenuated strain HZ2 (adapted to growth in DF-1 cells), which was propagated in DF-1 cells and concentrated by ultracentrifugation, was a gift from Dr. Yaowei Huang (36). Mouse anti-Flag and anti-His mAbs, mouse anti-dsRNA mAb, and rabbit pAb against glyceraldehyde-3-phosphate dehydrogenase (GAPDH) were purchased from MilliporeSigma (Burlington, MA, USA), Scicons (Szirák, Hungary), and GoodHere Biotechnology (Hangzhou, China), respectively. Rabbit anti-eIF2α, anti-p-eIF2α(Ser51), and anti-PKR antibodies were purchased from Cell Signaling Technology (Danvers, MA, USA). Rabbit anti–p-PKR(Thr41) antibody was purchased from Thermo Fisher Scientific. Rabbit anti-STAU1 and anti-G3BP1 antibodies were supplied by Proteintech (Wuhan, China). Mouse anti-VP1 and anti-VP3 polyclonal antibodies were generated as previously described (37). Alexa Fluor-568–labeled goat anti-mouse IgG was purchased from Thermo Fisher Scientific, and DAPI was purchased from Merck Millipore (Billerica, MA, USA).

Virus infection and Western-blot analysis

The cells were mock-infected or infected with concentrated IBDV at 37°C, and lysed in the lysis buffer (50 mM Tris-HCl [pH 7.4], 150 mM NaCl, 1% Triton X-100, and a protease inhibitor cocktail) at the indicated time. After centrifugation at 12,000 *g* for 30 min at 4°C, the supernatant was collected to prepare the samples with the loading buffer. Equivalent amounts of cell lysate were subjected to 12% SDS-PAGE and transferred to nitrocellulose membranes, and then blotted as previously described (23, 37). Finally, the blots were scanned and densitometric analysis was performed by using Quantity One software (Bio-Rad, Hercules, CA, USA).

Plasmids and transfection

The amplification of the full length of chSTAU1 and the generation of Flag-chSTAU1 and the derived mutant plasmid were performed by the method as previously described (37). All the constructs were confirmed by Sanger sequencing. Cell transfection was performed by using the Lipofectamine 2000 reagent

(Thermo Fisher Scientific) according to the manufacturer's instructions.

Immunoprecipitation RT-PCR

The immunoprecipitation (IP) RT-PCR assay was performed as previously described (38). Briefly, the HEK293T cells in the 6-well plate was transfected with Flag-chSTAU1 or vector for 24 h; after the cells were mock-infected or infected with IBDV (MOI 5) for another 12 h, the whole cell lysate was extracted with 500 μl lysis buffer. After preclearing with 30 μl protein A/G-agarose (GE Healthcare, Waukesha, WI, USA), the supernatant was incubated with 1 μg anti-Flag and 30 μl protein A/G-agarose. After 6 h of incubation, beads were washed 5 times with lysis buffer and resuspended in 200 μl lysis buffer with 0.1% SDS and 50 μg proteinase K. The RNA was recovered after digestion, phenol–chloroform–isoamyl alcohol extraction and ethanol precipitation, and reverse transcription reaction was performed by using a SuperScript first-strand synthesis system (Fermentas, Pittsburgh, PA, USA) according to the manufacturer's instructions. PCR was performed according to a standard protocol. The primers (5′-CATTGAAGGCGTGCGAGAAGAC-3′, 5′-GCATTGAGGGCTCCCGTCATAG-3′) were used for IP RT-PCR amplification of *vp4*.

RNA interference

The sequences of the 3 vector-based shRNAs targeting different regions of chicken STAU1 mRNA transcript were: 5′-GGATGAGATCTACTTACAACT-3′ (shSTAU1.1), 5′-GCTTCCTGCTGGAATTCTTCC-3′ (shSTAU1.2), and 5′-GCTCATTCAAAGGTGTTTACA-3′ (shSTAU1.3). The sequence of shRNA against human STAU1 was 5′-AAATAGCACAGTTTGGAAACT-3′ as previously reported (39). The details of the RNA interference have been previously described (23, 37).

Preparation of chSTAU1/(1–468) in *Escherichia coli*

Recombinant His-tagged chSTAU1/(1–468) were produced in *E. coli* strain BL21. Following transformation of pET28a-chSTAU1/(1–468), exponentially growing cultures were induced with 1 mM isopropyl-1-thio-β-D-galactopyranoside for 6 h at 30°C with shaking (100 rpm). Bacterial cell pellets containing recombinant His fusion proteins were resuspended in 10 ml of buffer B [8 M urea, 100 mM NaH_2PO_4, and 100 mM Tris·HCl (pH = 8.0)]. The extracts were sonicated, incubated on ice for 20 min, and then clarified by centrifugation. Recombinant proteins were extracted from the lysate using nickel nitrilotriacetic acid–agarose (Qiagen, Germantown, MD, USA), followed by washing with buffer C [8 M urea, 100 mM NaH_2PO_4, and 100 mM Tris·HCl (pH = 6.3)] and buffer D [8 M urea, 100 mM NaH_2PO_4, and 100 mM Tris·HCl (pH = 5.9)]. The fusion protein was eluted PBS containing 250 mM of imidazole.

IBDV dsRNA pulldown assay

IBDV genomic dsRNA extraction was performed as previously described (12, 40), and the purified IBDV genomic dsRNA was conjugated with biotin by UV irradiation (365 nm) as previously described (41). Biotin-labeled IBDV dsRNA was either added to whole cell lysates or incubated with *E. coli*–produced recombinant His-chSTAU1/(1–468). The mixtures were incubated on a rotator at 4°C for 2 h, and subsequently 20 μl of streptavidin-agarose was added for another 1 h at 4°C with agitation. The final mixture was then rinsed 5 times with lysis buffer to reduce nonspecific binding. The precipitates were separated on SDS–polyacrylamide gels, transferred onto nitrocellulose membranes, and processed for Western blot analysis.

dsRNA IP

The monolayer of DF-1 cells in the 6-well plate were mock-infected or infected with IBDV (MOI 1) for 6, 12, or 18 h. After infection, cells were washed twice with cold PBS and lysed in IP buffer [20 mM Tris (pH 7.4), 150 mM NaCl, 2 mM EDTA, and 1% Triton X-100] containing protease inhibitor cocktail and 100 U/ml RNase inhibitor (Thermo Fisher Scientific) on ice for 30 min with frequent agitation. Lysates were centrifuged for 10 min at 13,000 *g* at 4°C, and the supernatant was collected. The supernatant was incubated with 2 μg of J2 mAb for 3 h at 4°C on a rotating wheel and then with 20 μl of 50% slurry protein G agarose beads (GE Healthcare) for 3 h at 4°C. The beads were washed 5 times with IP buffer, and proteins were eluted by boiling in reducing sample buffer. Finally, the samples were subjected to SDS-PAGE and Western blot analysis with the corresponding antibodies.

Gel shift assay

Purified IBDV genomic dsRNA (2 μg in each tube) was incubated with *E. coli*–produced recombinant His-chSTAU1/(1–468) (0, 1, 5, or 25 μg) in 200 μl total volume of lysis buffer for 1 h at 4°C; 20 μl samples from each tube were then subjected to 0.8% agarose gel electrophoresis with the voltage of 5 V/cm. The image was taken under the Gel Documentation and Imaging Analysis System (SAGE Tech, Beijing, China).

Dual luciferase assay

DF-1 cells stably expressing shRNA against enhanced green fluorescent protein (EGFP) or chSTAU1 in 48-well plates were transfected with pGL3–chIFN-β (200 ng/well) and pRL-TK (10 ng/well) together with 200 ng/well of various plasmids for 36 h. The resulting cells were transfected with IBDV dsRNA (1 μg/well) for 8 h for intracellular stimulation; alternatively, the resulting cells were mock-infected or infected with IBDV (MOI 5) for 8 h. The luciferase activity was measured by using the Luciferase Reporter Gene Assay Kit according to the manufacture's protocol (Beyotime, Nantong, China).

Plaque assay

The process of plaque assay was previously described (37).

qRT-PCR

The qRT-PCR was performed as described previously (37). The following primers were used for the qRT-PCR: GAPDH-F: 5′-CCCAGCAACATCAAATGGGCAGAT-3′; GAPDH-R: 5′-TGATAACACGCTTAGCACCACCCT-3′; IBDV-F: 5′-GGATACGATCGGTCTGACCCC-3′; and IBDV-R: 5′-TGATAGCGTTATAGAAGGAGGAGTTC-3′.

Indirect immunofluorescence assay and laser confocal scanning microscopy

DF-1 cells in chamber slides were transfected indicated plasmids for 24 h and then inoculated with IBDV (MOI 1) for another 12 h.

The cells were fixed in 4% formaldehyde solution for 1 h at 4°C and permeabilized with 0.1% TritonX-100. After extensive washing, the cells were stained sequentially with mouse anti-dsRNA antibody for 1 h at 37°C and Alexa Fluor-568– conjugated goat anti-mouse IgG for another 1 h at 37°C. For G3BP1 staining, DF-1 cells were transfected with EGFP-chSTAU1/wt, and either mock-infected or infected with IBDV (MOI 1) for 12 h. Cells were fixed and stained sequentially with mouse anti-dsRNA antibody and rabbit anti-G3BP1 antibody for 1 h at 37°C, followed by incubation with Alexa Fluor-568–conjugated goat anti-mouse IgG and Alexa Fluor-647–conjugated goat anti-rabbit IgG for another 1 h at 37°C. Nuclei were stained with DAPI (blue). Confocal imaging was done with a Zeiss LSM 880 Airyscan microscope using Zen software (Carl Zeiss, Oberkochen, Germany). All images were collected by using a ×63 Plan-Apochromat oil immersion objective. The number and size of dsRNA puncta were measured by using ImageJ software (National Institutes of Health, Bethesda, MD, USA). The colocalization analysis of dsRNA with EGFP-STAU1/wt or EGFP-STAU1/(469–702) was performed by calculating the Pearson's correlation coefficients using the Pearson-Spearman correlation colocalization plugin of ImageJ software as previously described (42). The fluorescence signal intensity was analyzed by using ImageJ software with 6 images/group, which contains 200 cells/field.

Statistical analysis

All data are presented as means ± SD for each group and were analyzed by using SPSS v.13.0 (IBM Corporation, Armonk, NY, USA). Student's *t* test was used for comparisons between 2 groups. Statistical significance was set at values of $P < 0.05$.

RESULTS

The IBDV genomic dsRNA interacts with the N-terminal moiety of STAU1

STAU1, a dsRNA-binding protein, has been involved in diverse gene expression pathways (43). To investigate whether IBDV genomic dsRNA could also be recognized by host cellular STAU1, the IBDV dsRNA pulldown assay was performed. Biotin-labeled IBDV dsRNA was incubated with whole chicken fibroblast DF-1 cell lysates, followed by a streptavidin-agarose pulldown. Endogenous chSTAU1 was precipitated by biotin-labeled IBDV dsRNA but not by the unlabeled dsRNA control (**Fig. 1*A***, lane *1 vs.* lane *2*). Seven unique peptides of STAU1 were identified in the IBDV dsRNA pulldown precipitate according to liquid chromatography tandem-mass spectrometry analysis (**Table 1**). We further assessed whether IBDV dsRNA could interact with the ectopically expressed STAU1. Whole cell lysates of HEK293T cells transfected with Flag-tagged chSTAU1, chMDA5, or chMAVS were subjected to IBDV dsRNA pulldown assays. chSTAU1 was readily pulled down by purified IBDV dsRNA (Fig. 1*Ba*, lane *3*), whereas chMDA5 and chMAVS were served as the positive and negative control (Fig. 1*Ba*, lanes *1* and *2*) for IBDV dsRNA binding, as previously reported (23).

To further confirm the observed interaction between IBDV dsRNA and chSTAU1, conversely, we used chSTAU1 as the bait for pull-down of viral dsRNA in IBDV-infected cells. HEK 293T cells were transfected with either empty vector or the Flag-chSTAU1, followed by IBDV or mock infection. Cell lysates were extracted and subjected to IP by using anti-Flag antibody, and an RT-PCR assay based on specific amplification of a fragment of *vp4* was used to reveal the presence of IBDV dsRNA in the precipitates. As shown in Fig. 1*Bb*, the specific RT-PCR–amplified *vp4* fragment was present in the anti-Flag precipitate from cells transfected with Flag-chSTAU1 and with IBDV infection (lane *4*) but not in that from cells transfected with empty vector with or without IBDV infection (lanes *1* and *2*), or transfected with Flag-chSTAU1 but without IBDV infection (lane *3*). Moreover, to investigate the interaction between endogenous chSTAU1 and IBDV dsRNA in virus-infected cells, coimmunoprecipitation assays were performed. Whole cell lysates of DF-1 cells either mock-infected or infected with IBDV were extracted at different time points postinfection, and IBDV dsRNA in the cell extracts was immunoprecipitated by using an anti-dsRNA antibody, followed by Western blot analysis using antibodies against chSTAU1 and VP3. As shown in Fig. 1*C*, endogenous chSTAU1 was detected after IP from IBDV-infected cells at 12 and 18 h postinfection but not from the mock-infected cells (lanes *3* and *4 vs.* lane *1*, upper panel of the anti-dsRNA IP panel) using anti-dsRNA antibody. As a positive control, VP3, the viral dsRNA-interacting protein, was concurrently coprecipitated by anti-dsRNA antibody from the virus-infected cells (lanes *3* and *4*, lower panel of the anti-dsRNA IP panel). Together, these data suggest that IBDV genomic dsRNA interacts with host cellular STAU1 *in vitro* and *in vivo*.

To identify the regions in chSTAU1 responsible for IBDV dsRNA binding, we generated various Flag-chSTAU1 mutants *via* deletion and truncation mutagenesis. The effects of various alterations in chSTAU1 on IBDV dsRNA binding were determined by using an IBDV dsRNA pulldown assay. As shown in the top panel of Fig. 1*D*, the mutant chSTAU1/(1–468) with the deletion of the C-terminal moiety of chSTAU1 (residues 469–702) exhibited the IBDV dsRNA binding in a level comparable to that of wild type (lane *4 vs.* lane *1*). The other mutants with different deletions displayed various levels in the IBDV dsRNA binding (lanes *2*, *3*, *5*, *6*, and *8*). By contrast, when the N-terminal moiety of chSTAU1 (residues 1–468) was removed from chSTAU1, the resulting mutant chSTAU1/(469–702) completely lost the ability to bind to IBDV dsRNA (lane *7*); this scenario shows that although the C terminus of chSTAU1 encompassing residues 469–702 is not involved in the IBDV dsRNA–binding activity, the N-terminal moiety of chSTAU1 (residues 1–468) is the region responsible for the IBDV dsRNA binding.

To further evaluate the importance of the N-terminal moiety of chSTAU1 in IBDV dsRNA binding, the isolated N-terminal chSTAU1 (residues 1–468) was used for the *in vitro* IBDV dsRNA pulldown assay and the gel shift assay. Purified recombinant His-chSTAU1/(1–468) and the positive control His-VP3 but not the His-GAPDH were precipitated by IBDV genomic dsRNA, as confirmed by immunoblotting with anti-His antibody (Fig. 1*Ea*). In the gel shift assay, incubation of purified IBDV genomic dsRNA with various concentrations of chSTAU1/(1–468) caused a typical smear-like shifting pattern of the dsRNA probe in agarose gel electrophoresis. The extent of

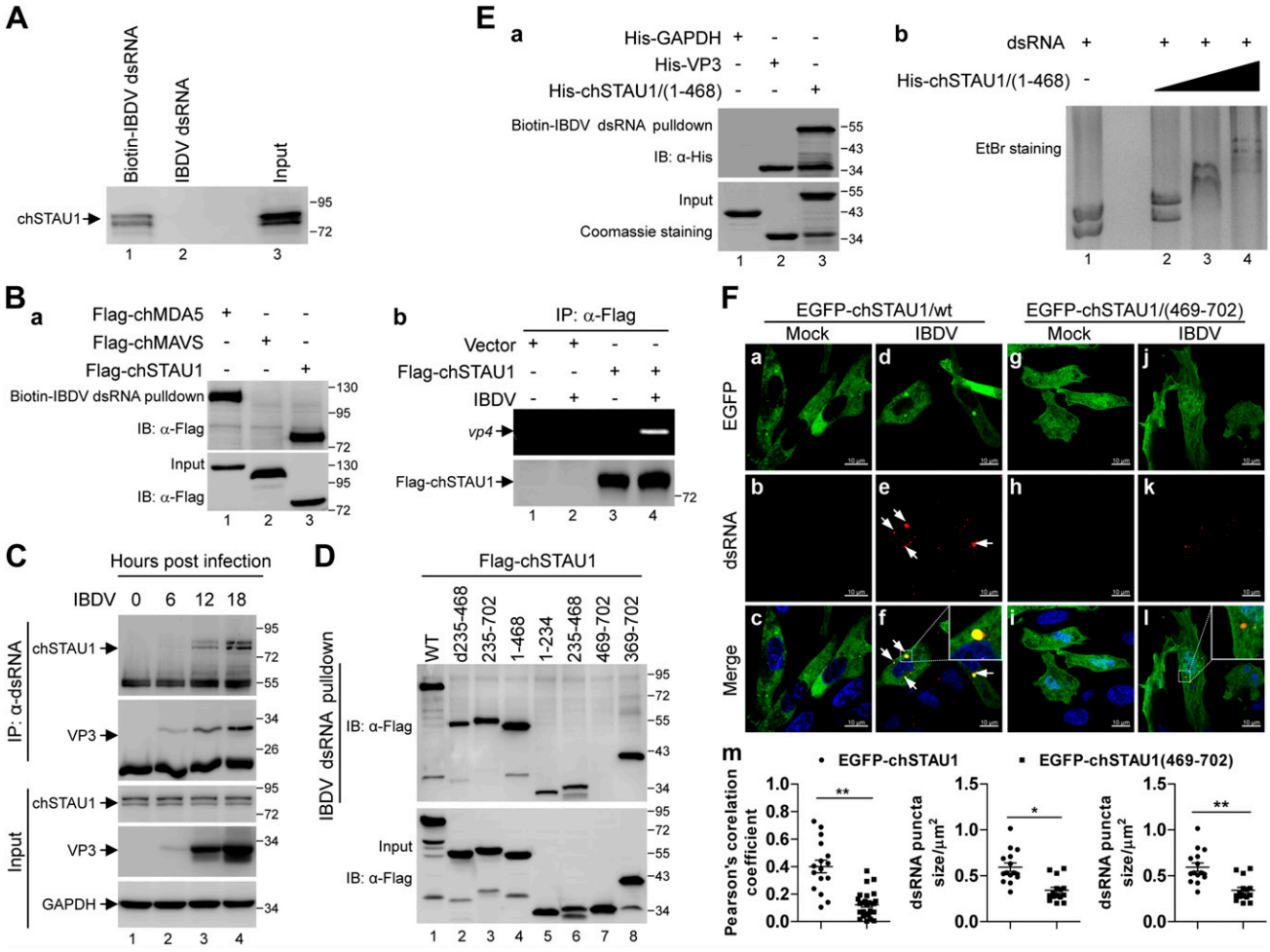

Figure 1. Intracellular STAU1 binds IBDV genomic dsRNA. *A*) IBDV genomic dsRNA interacts with host STAU1. Endogenous chSTAU1 was pulled down by IBDV genomic dsRNA. Whole cell lysates of DF-1 cells were prepared and incubated with either biotin-labeled IBDV genomic dsRNA (lane *1*) or unlabeled IBDV genomic dsRNA as a control (lane *2*), followed by pull-down with streptavidin-agarose beads. The precipitates were then analyzed by Western blot using the anti-STAU1 antibody. The whole cell lysate input (1:50) was used as positive control (lane *3*). *B*) Ectopically expressed chSTAU1 was pulled down by IBDV dsRNA. *Ba*) The whole cell lysates of HEK293T cells transfected with Flag-chSTAU1, Flag-chMDA5 (positive control), or Flag-chMAVS (negative control) were prepared and subjected to the IBDV dsRNA pull-down assay. The precipitates (upper panel) or whole cell lysate input (1:50) (lower panel) were analyzed by Western blot using the anti-Flag antibody. *Bb*) IBDV dsRNA was pulled down by Flag-chSTAU1 in IBDV-infected cells. HEK293T cells were transfected with the indicated plasmids, followed by IBDV or mock infection. The whole cell lysates were extracted and subjected to IP by using an anti-Flag antibody, and IP RT-PCR assay was performed to detect the presence of IBDV dsRNA in the precipitate. The expression of Flag-chSTAU1 in cell lysates from transfected cells was confirmed by Western blot by using anti-Flag (lower panel). *C*) IBDV dsRNA coimmunoprecipitation analysis of endogenous chSTAU1. DF-1 cells were infected with IBDV at MOI 1 and the cells were then collected at different time points as indicated postinfection. Coimmunoprecipitation assay was performed by using an anti-dsRNA antibody, followed by Western blot analysis using antibodies against STAU1 and VP3. *D*) Mapping of the IBDV dsRNA–binding region of chSTAU1. The whole cell lysates from the HEK293T cells ectopically expressing chSTAU1 or its deletion mutants were prepared and subjected to the IBDV dsRNA pull-down assay. Flag-tagged chSTAU1 pulled down by dsRNA (top panel) or in the whole cell lysate inputs (1:50) (bottom panel) was analyzed by Western blot with the anti-Flag antibody. *E*) *E. coli*–produced recombinant chSTAU1 was pulled down by IBDV genomic dsRNA *in vitro*. *Ea*) His tagged *E. coli*–produced GAPDH, VP3, and chSTAU1/(1–468) protein (100 μg each) were subjected to the IBDV dsRNA pull-down assay (upper panel), and the input (1:20) proteins used for dsRNA pulldown assay were evaluated by using Coomassie blue staining (lower panel). *Eb*) Gel-shift assay of the interaction between the N-terminal moiety of chSTAU1 (residues 1–468) and IBDV dsRNA; 10 μg IBDV genomic dsRNA was incubated with increasing amounts of His-tagged recombinant N-terminal moiety of chSTAU1/(1–468) (0, 1, 5, and 25 μg) at 4°C for 1 h. One tenth of each reaction mixture was subjected to 0.8% agarose gel electrophoresis. *F*) (*Fa–Fl*) Representative immunofluorescence images of mock-infected or IBDV-infected DF-1 cells transfected with either EGFP-chSTAU1/wt or EGFP-chSTAU1/(469–702) (green), and immunostained with anti-dsRNA (red). Nuclei were stained with DAPI (blue). White arrowheads indicate dsRNA puncta that colocalized with EGFP puncta. Magnification of the overlapping fluorescent puncta is shown in the inset. Scale bars, 10 μm. *Fm*) Quantification of the Pearson's correlation coefficient values of the overlap of dsRNA and EGFP-chSTAU1/wt or EGFP-chSTAU1/(469–702) (left), dsRNA fluorescent puncta number (middle) and size (right) in IBDV-infected DF-1 cells. $N = 15$–20 images/condition, 3 experiments; mean ± SD. $^*P < 0.05$, $^{**}P < 0.01$.

TABLE 1. *The unique peptide sequence of chSTAU1 identified in the precipitate pulled down by IBDV dsRNA from the DF-1 lysate*

Number	Identified unique peptide
1	LLSEQGPAHSK
2	VSVGEFMGEGEGK
3	NAAIAVLEELKKLPPLPTVEK
4	LQTSPEYGQGMNPISR
5	NAAENMLEILGFK
6	VTFFEPGSEETSTSNKEDEFR
7	LLSELDQQTTEMPR

chSTAU1-dsRNA complex formation was increased with the increment of concentration of chSTAU1 (Fig. 1*Eb*, lanes *2–4*). To examine whether the localization of cellular chSTAU1 is relevant to the distribution of IBDV dsRNA in the viral infected cells, DF-1 cells that had been transfected with pEGFP-chSTAU1/wt or the dsRNA-binding deficient mutant pEGFP-chSTAU1/(469–702) and subsequently infected with IBDV were immunostained with the anti-dsRNA antibody. The confocal microscopy images revealed that IBDV dsRNA (red) was predominantly detected in the cytosol and displayed a pattern of small fluorescent puncta in IBDV-infected cells (Fig. 1*Fe* and *Fk*), which was not seen in the DF-1 cells without IBDV infection as the negative controls (Fig. 1*Fb* and F*h*). Although some EGFP-chSTAU1/wt (green) was diffusely distributed in cytosol, some of the protein formed small cytosolic puncta, which is consistent with earlier observations (44). Importantly, the chSTAU1 puncta exhibited a substantial degree of colocalization with IBDV dsRNA puncta in IBDV-infected cells with concurrent transfection of EGFP-chSTAU1/wt (Fig. 1*Ff*-merge; the inset in *f*). The IBDV dsRNA-binding deficient mutant EGFP-chSTAU1/(469–702) was diffusely distributed in both the cytosol and nuclear. However, remarkably, the number per cells and the average size of the red punctate fluorescent signals representing mainly IBDV dsRNA was markedly reduced in the IBDV-infected cells expressing the mutant chSTAU1/(469–702) compared with the virus-infected cells expressing chSTAU1/wt (Fig. 1*Fm*). Furthermore, the overall colocalization between chSTAU1/wt and IBDV dsRNA in the virus-infected cells was 0.4 but only 0.13 for chSTAU1/(469–702) with the viral dsRNA as analyzed by using Pearson's correlation coefficient (Fig. 1*Fm*). Together, these data show that IBDV dsRNA interacts directly with host cellular chSTAU1 *in vitro via* the N-terminal moiety of chSTAU1 (aa 1–468), and IBDV dsRNA and chSTAU1 can be recruited and localized to the same protein puncta in the IBDV infection. Many viruses induce SGs during the course of infection, which are sites of stalled translation initiation complexes (45), and STAU1 is recruited and localized to SGs (46). To investigate whether IBDV promotes the formation of SGs and whether these punctate fluorescence signals of IBDV dsRNA and EGFP-STAU1 are localized to SGs, the SG assembly was assessed by the punctate G3BP1 staining pattern. As shown in Supplemental Fig. 1, the formation of a visible SG was rarely observed in either the mock- or IBDV-infected DF-1 cells that expressed EGFP-chSTAU1/wt. Moreover, the overlap of EGFP-STAU1/wt and IBDV dsRNA puncta was not enriched in the cellular localization of G3BP1 in IBDV-infected DF-1 cells.

IBDV dsRNA- STAU1 interaction potentiates the viral productive replication

Having shown that IBDV genomic dsRNA interacts with STAU1, we next examined the role of STAU1 in IBDV productive replication by assessing the effect of chSTAU1 knockdown on IBDV proliferation in DF-1 cells. First, we screened for the highly efficient shRNA that potently down-regulates chSTAU1. Expression of 2 shRNAs (clone shSTAU1.1 and clone shSTAU1.3) resulted in a decrease of >80% for the ectopically expressed Flag-chSTAU1 in HEK293T cells compared with that of the control non-targeting shRNA against EGFP (shEGFP) (lanes *2* and *4 vs.* lane *1* in *a* of **Fig. 2*A***). The stable DF-1 cells expressing shRNA1.1 *via* a lentivirus-mediated approach were then established, in which expression of endogenous chSTAU1 was down-regulated by >80% (Fig. 2*Ab*). Surprisingly, expression of the major viral proteins, including both VP1 and VP3, was significantly reduced (>70%) at 18 h post-infection (hpi) in chSTAU1 knockdown DF-1 cells infected with IBDV compared with that in shEGFP-expressing DF-1 cells (Fig. 2*B*, lane *8 vs.* lane *7*). Consistent with the Western blot result, immunostaining using anti-VP3 antibody found that the VP3 signal (green) was much weaker in chSTAU1 knockdown cells than that in control cells (Fig. 2*Ca vs. b*). The quantified relative fluorescent intensity results showed that chSTAU1 knockdown led to a decrease of >60% in VP3 (Fig. 2*Cc*). Furthermore, a plaque assay was performed to assess the effect of chSTAU1 knockdown on IBDV replication. As shown in Fig. 2*D*, at 1 and 6 hpi, there was no significant difference in viral titer between chSTAU1 knockdown cells and control cells; however, at 12 hpi, the viral titer was 50% lower in chSTAU1 knockdown cells (10,000 PFU/ml *vs.* 20,000 PFU/ml) and 85% lower at 18 hpi (30,000 PFU/ml *vs.* 20,0000 PFU/ml) compared with the control cells. Moreover, qRT-PCR analysis showed that the relative IBDV genome copy number in chSTAU1 knockdown cells was also significantly reduced by ~50% at 12 hpi and 80% at 18 hpi relative to the control cells (Fig. 2*E*). Thus, these data support that down-regulation of host chSTAU1 impairs IBDV productive replication at the late stage of viral infection.

We next examined the effect of chSTAU1 overexpression on IBDV replication. The expression of viral proteins VP1 and VP3 were increased by >3-fold in cells overexpressing Flag-chSTAU1 but not the IBDV dsRNA–binding deficient Flag-chSTAU1/(469–702), compared with that in cells expressing vector control (**Fig. 3*A***, lanes *4* and *3 vs.* lanes *2*). Furthermore, overexpression of chSTAU1 led to an increase of ~3-fold at 12 hpi and 5-fold at 18 hpi in the relative level of the IBDV genome as measured by using qRT-PCR (Fig. 3*B*) and an increase of nearly 6-fold in the viral titer as measured by plaque assay at 18 hpi (Fig. 3*C*), relative to the vector control.

These data thus suggest that chSTAU1 promotes the productive replication of IBDV, which is dependent on the interaction between IBDV genomic dsRNA and chSTAU1.

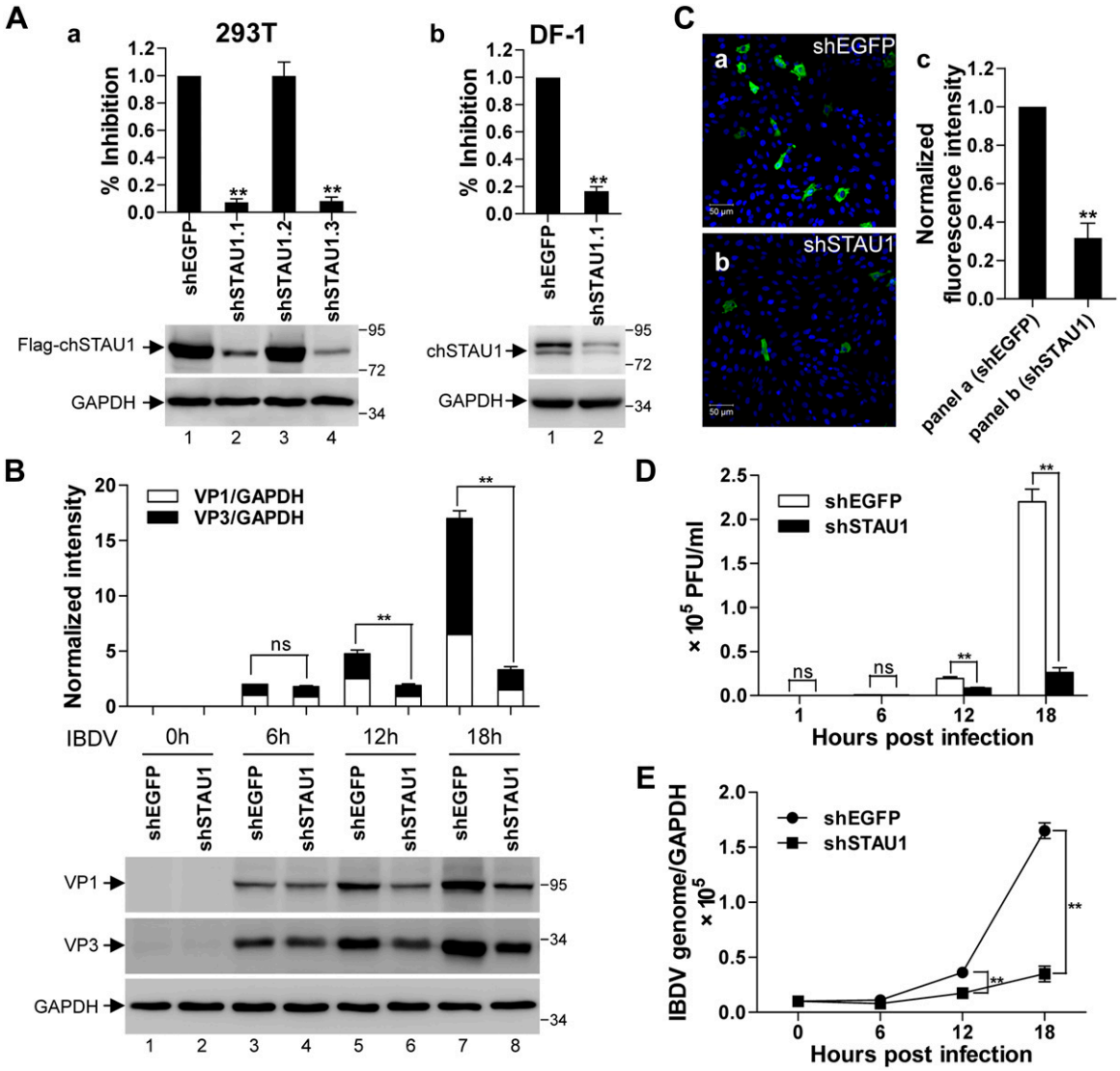

Figure 2. Down-regulation of STAU1 impairs IBDV productive replication. *A*) Selection of shRNA sequences that are effective in down-regulating the expression of chSTAU1. *Aa*) Three independent shRNAs designed against different sequences of chSTAU1 were cotransfected with Flag-chSTAU1 into HEK293T cells for 48 h. The whole cell lysates were extracted and subjected to Western blot with an anti-Flag antibody (middle panel) to determine the efficacy of chSTAU1 knockdown. The anti-GAPDH antibody (lower panel) was used as the internal control. The histogram was plotted based on the quantified data from 3 independent assays using Quantity One software (upper panel). *Ab*) Endogenous chSTAU1 protein knockdown in DF-1 cells stably expressing the effective shRNA from *Aa*. *B*) chSTAU1 knockdown led to a reduced IBDV proliferation as assessed by Western blot analysis of the levels of viral proteins. Either chSTAU1 knockdown DF-1 cells (shSTAU1) or mock knockdown control DF-1 cells (shEGFP) were either mock-treated or infected with IBDV (MOI 1) for 6, 12, or 18 h, as indicated. Whole cell lysates were extracted and subjected to Western blot analysis by using anti-VP1 and anti-VP3 antibodies. Anti-GAPDH was used as the internal control. The histogram was plotted based on the quantified data from 3 independent assays using Quantity One software (top panel). *C*) chSTAU1 knockdown led to a reduction in the IBDV proliferation as assessed by immunofluorescence assay. chSTAU1 knockdown control DF-1 cells (*Ca*) or knockdown DF-1 cells (*Cb*) were infected with IBDV (MOI 1) for 12 h and costained with DAPI (blue) and anti-VP3 (green), and proceeded to laser confocal scanning microscopy analysis. Scale bars, 50 μm. *Cc*) The bar graph indicates the normalized fluorescence intensity of images from (*Ca*, *Cb*). Mean intensity and cell number in each image were measured by using ImageJ software, and the normalized fluorescence intensity was calculated and plotted in the bar graph. $N = 6$ images/condition. *D*) Down-regulation of chSTAU1 impaired IBDV replication but not internalization. Stable chSTAU1 knockdown DF-1 cells or knockdown control DF-1 cells were infected with IBDV (MOI 1) for 1, 6, 12, and 18 h, as indicated. Cell homogenates were then extracted and used for the plaque assay to assess the intracellular virus titer. The histogram was plotted based on 3 independent experiments. *E*) Down-regulation of chSTAU1 inhibits IBDV genome replication as measured by qRT-PCR. Stable chSTAU1 knockdown DF-1 cells or knockdown control DF-1 cells were infected with IBDV (MOI 1) for 0, 6, 12, and 18 h, as indicated. For assessing IBDV replication, total RNA was extracted and subjected to qRT-PCR analysis of the 5′ UTR of segment A. Results were normalized to GAPDH mRNA in the same samples. The histogram was plotted based on 3 independent experiments. Ns, not significant. $^{**}P < 0.01$.

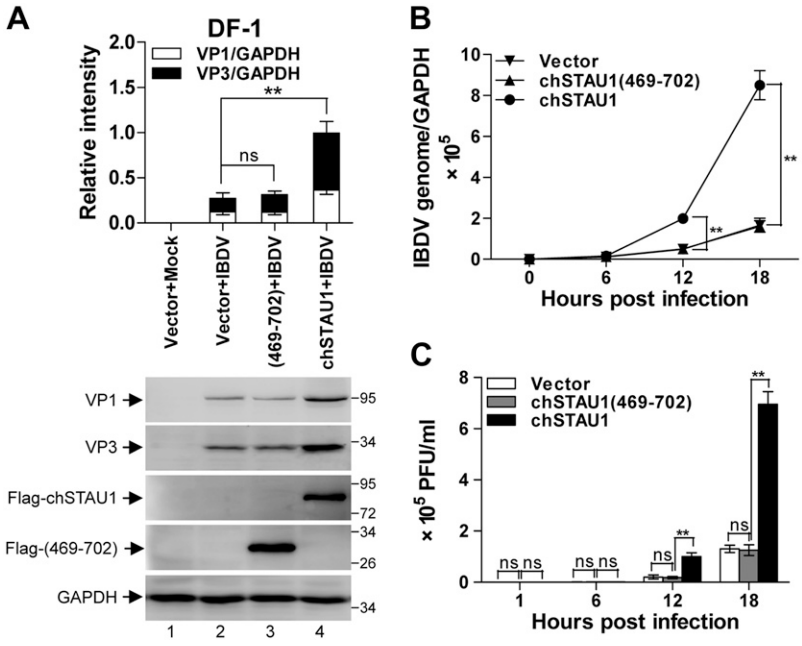

Figure 3. Overexpression of STAU1 promotes IBDV replication. DF-1 cells were transfected with the indicated plasmids for 24 h, followed by inoculation with IBDV (MOI 1) for another 12 h. *A*) Overexpression of chSTAU1 facilitated the expression of VP1 and VP3. Whole cell lysates were prepared and Western blot analysis was conducted by using antibodies against VP1, VP3, GAPDH, and chSTAU1, as indicated (lower panel). The histogram shows the quantification of VP1 and VP3 normalized to GAPDH from 3 independent assays (upper panel). *B*) The effect of overexpression of chSTAU1 or chSTAU1/(469–702) on IBDV replication was measured according to qRT-PCR analysis. Total RNA of infected cells was extracted at the indicated time point postinfection, and qRT-PCR analysis was conducted to assess the replication of IBDV by amplifying the 5′ UTR of segment A. *C*) The effect of overexpression of chSTAU1 or chSTAU1/(469–702) on IBDV replication as measured according to plaque assay. Cell homogenates of infected cells were extracted at the indicated time postinfection to perform the plaque assay to assess the intracellular virus titer. All data are presented as means ± SD from at least 3 independent experiments. Ns, not significant. $^{**}P < 0.01$.

IBDV dsRNA–STAU1 interaction counteracts IBDV infection–induced IFN-β transcription

We next attempted to elucidate the mechanism underlying the action of the IBDV dsRNA–STAU1 interaction in promoting IBDV replication. Type I IFN (IFN-α/β) is one of the major cytokines rapidly triggered by many viruses, and it plays a critical role in antiviral response (*e.g.*, inhibiting viral replication) (47). IBDV dsRNA could be sensed by the cytoplasmic PRR MDA5 to induce the production of IFN-β in DF-1 cells (23, 48). To assess whether the chSTAU1–dsRNA interaction may modulate the IFN-β induction in host cells, resulting in the regulation of IBDV replication, we compared the activity of a chIFN-β promoter-driven luciferase reporter gene after IBDV infection between chSTAU1 knockdown DF-1 cells and in the nontargeting control shEGFP cells. In line with a previous report (23), IBDV dsRNA stimulated the transcriptional activity of the chIFN-β promoter expressed as relative luciferase units (**Fig. 4*A***, bar 5 *vs.* bar 1). Significantly, knockdown of chSTAU1 increased the activity of the chIFN-β promoter induced by IBDV genomic dsRNA and poly (I:C) by >2-fold (Fig. 4*A*, bar 6 *vs.* bar 5 and bar 4 *vs.* bar 3, respectively). RT-PCR analysis of the chIFN-β mRNA showed that knockdown of chSTAU1 significantly enhanced the level of chIFN-β mRNA responsive to intracellular IBDV dsRNA stimulation (Fig. 4*B*, lane *4 vs.* lane *2* in the chIFN-β indicated panel). In contrast to IFN-β responses, there was no obvious difference in chIFN-α mRNA levels between chSTAU1 knockdown and control DF-1 cells (Fig. 4*B*, lane *4 vs.* lane *2* in the chIFN-α indicated panel). Furthermore, the IBDV infection–induced activation of IFN-β promoter was also increased by >3-fold in chSTAU1 knockdown DF-1 cells compared with that in shEGFP control DF-1 cells (Fig. 4*C*, bar 4 *vs.* bar 2). These data suggest that chSTAU1 down-regulation selectively targets the induction of chIFN-β rather than chIFN-α in response to IBDV dsRNA stimulation or IBDV infection.

We also investigated the effect of chSTAU1 overexpression on the induction of chIFN-β by the intracellular IBDV dsRNA stimulation. As shown in Fig. 4*D*, overexpression of chSTAU1 reduced the induction of chIFN-β under the intracellular IBDV dsRNA stimulation (lane *4 vs.* lane *2* in the chIFN-β indicated panel). The effect of chSTAU1 overexpression on host chIFN-β responsive to IBDV dsRNA stimulation was further monitored with luciferase reporter assay by cotransfection of chIFN-β promoter reporter construct together with empty vector, chSTAU1/wt, or various chSTAU1 deletion mutants in DF-1 cells, stimulated with intracellular IBDV dsRNA or mock-treated. Overexpression of chSTAU1/wt or the chSTAU1 mutants that retain full or partial IBDV dsRNA–binding ability significantly decreased the chIFN-β promoter transcription responsive to IBDV dsRNA (Fig. 4*E* bars 4, 6, 8, 10, 12, and 14). By contrast, the dsRNA binding–deficient mutant chSTAU1/(469–702) failed to suppress the IBDV dsRNA–induced chIFN-β promoter transcription (Fig. 4*E*, bar 16). Interestingly, another chSTAU1/(369–702) that has IBDV dsRNA–binding capacity (as shown in lane *8* of Fig. 1*D*) was rendered the inhibitory effect again on the chIFN-β promoter transcription (Fig. 4*E*, bar 18).

PKR is an important mediator of IFN-β induction after infection by many RNA viruses (49). Ectopic expression of IBDV VP2 triggers the phosphorylation of PKR, and VP3 attenuates VP2-induced PKR activation (26). To determine the effect of silencing of STAU1 in the activation of PKR in IBDV infection, DF-1 cells were either mock- or

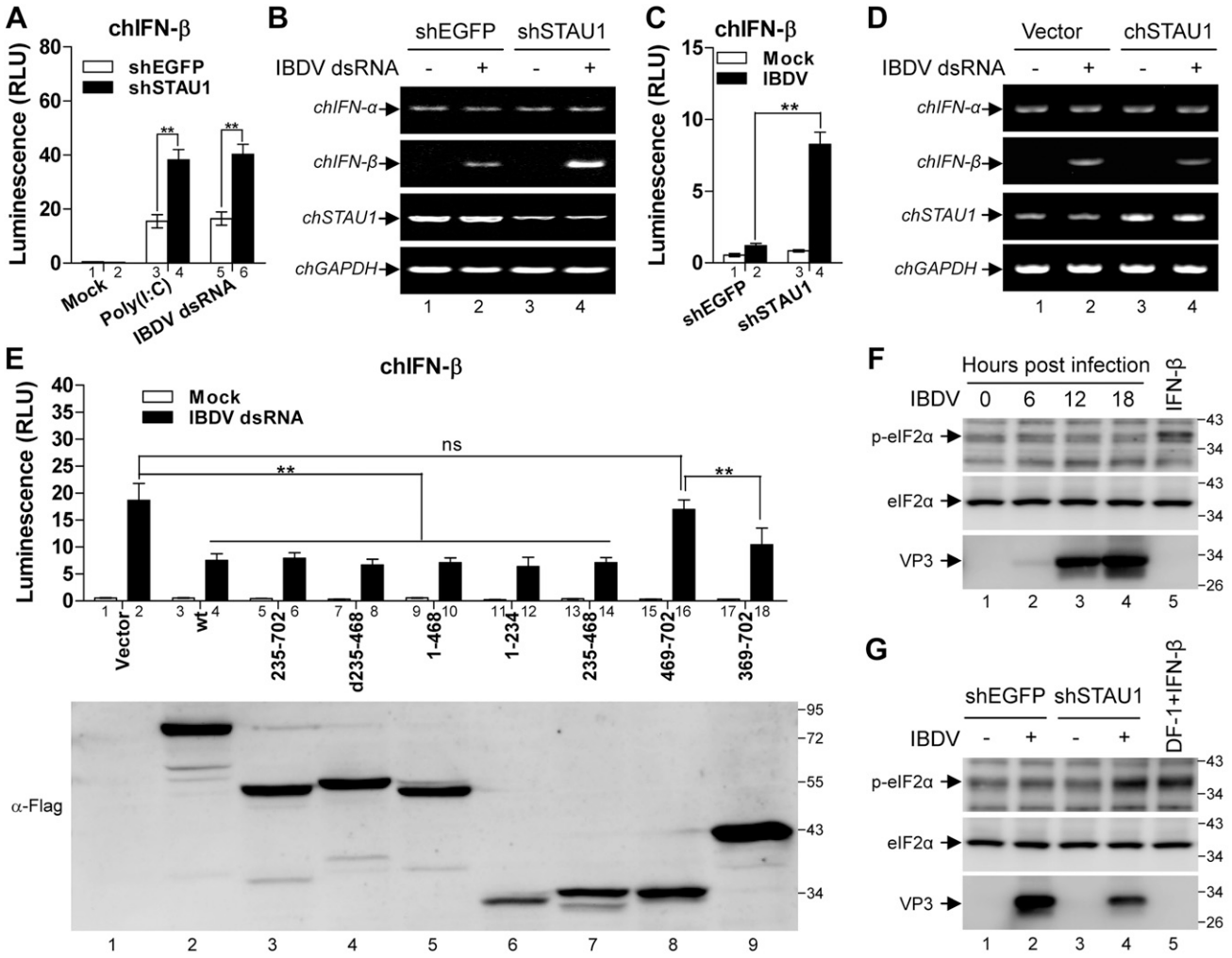

Figure 4. STAU1 inhibits IBDV dsRNA–induced IFN-β transcription. *A*) Down-regulation of chSTAU1 promotes chIFN-β promoter activity in response to intracellular dsRNA stimulation. DF-1 cells stably expressing shEGFP (open bars) or shSTAU1 (filled bars) were cotransfected with pGL3–chIFN-β luciferase reporter and pRL-TK for 36 h, and stimulated with mock, poly(I:C), or IBDV dsRNA for another 8 h. Luciferase activity was then assessed by using the dual-luciferase assay. *B*) Down-regulation of chSTAU1 led to an increase in mRNA level of chIFN-β but not chIFN-α in response to IBDV genomic dsRNA stimulation. DF-1 cells stably expressing shRNA against chSTAU1 or control shEGFP were intracellularly stimulated with IBDV dsRNA by transfection. The cells were harvested 8 hpi, and total RNA was extracted for RT-PCR. The amplification of the fragments of *chIFN-α*, *chIFN-β*, ch*STAU1*, and *chGAPDH* mRNA were subjected to 1.0% agarose gel electrophoresis analysis, as indicated. *C*) Down-regulation of chSTAU1 potentiates IBDV infection–induced activation of chIFN-β promoter. DF-1 cells with stable expression of shEGFP or shSTAU1 were cotransfected with pGL3–chIFN-β and pRL-TK for 36 h and then mock-infected or infected with IBDV (MOI 5) for another 8 h. The dual-luciferase assay was used to assess luciferase activity. *D*) Overexpression of chSTAU1 led to a decrease in mRNA level of chIFN-β but not chIFN-α in response to IBDV genomic dsRNA stimulation. DF-1 cells transiently expressing chSTAU1 or vector control were intracellularly stimulated with IBDV dsRNA by transfection. RT-PCR amplification of *chIFN-α*, *chIFN-β*, *chSTAU1*, and *chGAPDH* mRNA was performed the same as described in *B*. *E*) The IBDV dsRNA–induced activation of chIFN-β promoter is inhibited by overexpression of chSTAU1, which depends on the IBDV dsRNA–binding activity of chSTAU1. DF-1 cells were cotransfected with the indicated plasmids together with luciferase reporter plasmids pGL3–chIFN-β and pRL-TK for 36 h; the cells were either mock-stimulated (open bars) or intracellularly stimulated with IBDV genomic dsRNA (filled bars) for another 8 h. The dual-luciferase assay was used to assess luciferase activity. The histogram was plotted based on the results of 3 independent experiments. The expression of chSTAU1 wild-type and various mutants was verified by Western blot analysis using an anti-Flag antibody (lower panel). $^{**}P < 0.01$. *F*) eIF2α phosphorylation in response to IBDV infection. ShSTAU1 or control shEGFP DF-1 cells were mock infected or infected with IBDV for 12 h; cell lysates were analyzed by Western blot with antibodies against phosphorylated eIF2α, total eIF2α, and VP3.

IBDV-infected, and the activation of PKR was indirectly analyzed through the phosphorylation of its natural substrate eIF2α. Whole cell lysates from the infected cells were subjected to Western blot analysis with antibodies against phosphorylated eIF2α, eIF2α, and VP3. As shown in Fig. 4*F*, there were no significant differences in the phosphorylation levels of eIF2α between mock- and IBDV-infected cells over a time course of 18 h (lanes *1–4*), in contrast with cells treated with IFN-β as a positive control, in which the enhancement of eIF2α phosphorylation was clear (lane *5*). This outcome suggests that IBDV infection alone was unable to stimulate eIF2α phosphorylation.

Similarly, down-regulation of STAU1 alone hardly affected eIF2α phosphorylation either (Fig. 4*G*, lane *3 vs.* lane *1*). However, IBDV infection remarkably increased the level of eIF2α phosphorylation in cells wherein endogenous STAU1 was knocked down (Fig. 4*G*, lane *4 vs.* lane *2*), indicating that STAU1 plays a role in preventing IBDV infection to induce eIF2α activation.

Furthermore, we assessed the effect of down-regulation of STAU1 on the response of PKR phosphorylation to either ectopic expression of viral proteins VP2 and/or VP3 or to IBDV infection in HeLa cells. Consistent with a previous report (26), in mock shEGFP-transfected cells, ectopic expression of VP3 decreased the VP2-triggered PKR phosphorylation (Supplemental Fig. 2A, lane *3 vs.* lane *2*). This pattern of PKR phosphorylation from actions of ectopically expressed VP2 and/or VP3 was not affected upon knockdown of STAU1 (Supplemental Fig. 2A, lanes *4–6*). Interestingly, in response to IBDV infection (at both 6 and 12 hpi), PKR showed little change in phosphorylation in the mock control shEGFP cells (Supplemental Fig. 2B, lanes *2* and *3 vs.* lane *1*) but exhibited a significant increase in STAU1 knockdown cells (Supplemental Fig. 2B, lanes *5* and *6 vs.* lane *4*).

Together, these data indicate that IBDV dsRNA-STAU1 interaction inhibits the viral infection-induced host antiviral cytokine IFN-β induction, resulting in an enhancement of the viral proliferation.

Direct binding of STAU1 to IBDV dsRNA competes with the interaction of MDA5 with IBDV dsRNA, which dampens the MDA5-mediated IFN-β induction

MDA5, a cytoplasmic RNA helicase and a viral dsRNA sensor, recognizes and binds IBDV dsRNA to up-regulate the host IFN-β response to IBDV dsRNA stimulation (48). We thus assessed the effect of the chSTAU1–dsRNA interaction on chMDA5 binding to the IBDV dsRNA by using IBDV dsRNA pull-down assays. In agreement with the previous report (23) and with the result in Fig. 1, chMDA5 and chSTAU1 were readily pulled down by IBDV dsRNA (**Fig. 5*A***, band α in lane *1* and band β in lane *2*, respectively). When the IBDV dsRNA was incubated with the chMDA5 and chSTAU1 mixture, both chMDA5 and chSTAU1 could be concurrently pulled down by the viral dsRNA (Fig. 5*A*, bands α′ and β′ in lane *4*). Of note, interestingly, the amount of chMDA5 pulled down by IBDV dsRNA was reduced by ~60% in the presence of chSTAU1 compared with that in the absence of chSTAU1 (Fig. 5*A*, band α′ in lane *4*, *vs.* band α in lane *1*; the histogram in the right panel). The chSTAU1 mutant chSTAU1/(469–702), which is defective in IBDV dsRNA binding, failed to compete with chMDA5 (Fig. 5*A*, band α″ in lane *5*, *vs.* band α in lane *1*). This finding suggests that direct binding of STAU1 to IBDV dsRNA competes at least partially with the binding of MDA5 to IBDV dsRNA.

To further investigate the competition between chSTAU1 and MDA5 in binding to IBDV dsRNA, a direct *in vitro* competition assay was performed. Whole cell lysate from HEK293T cells either mock-transfected or transfected with Flag-chMDA5 was incubated with increasing amounts of recombinant His-chSTAU1/(1–468) from 1 to 9 μg, followed by a pull-down assay by using IBDV dsRNA. The pulled-down proteins were subjected to Western-blot analysis using antibodies against Flag and His. The binding of Flag-chMDA5 to the IBDV dsRNA was found to decrease with increasing amounts of recombinant His-chSTAU1/(1–468) (Fig. 5*B*), indicating that chSTAU1 can displace chMDA5 from the IBDV dsRNA.

We next determined whether chSTAU1 could serve as a competitive inhibitor of the chMDA5-mediated transcription of IFN-β by chIFN-β promoter-luciferase assay. The IBDV dsRNA–induced enhancement of chIFN-β promoter activity was significantly lowered by up to 2.5-fold in cells expressing shRNA against chMDA5 (shchMDA5) cells compared with the control shEGFP-expressing cells (Fig. 5*C*, bar 4 *vs.* bar 2), indicating that the IBDV dsRNA–induced enhancement of chIFN-β promoter activity is mainly mediated by endogenous chMDA5. Consistent with the result in Fig. 4*E*, overexpression of chSTAU1 led to an inhibition of dsRNA-mediated induction of chIFN-β promoter activity (Fig. 5*C*, bar 10 *vs.* bar 2), which was not observed with the overexpression of the IBDV dsRNA–binding deficient mutant chSTAU1/(469–702) (bar 6 *vs.* bar 2). Interestingly, overexpression of chSTAU1 together with shchMDA5 to knock down chMDA5 resulted in a >2.5-fold repression of dsRNA-induced chIFN-β promoter activity compared with that caused by overexpression of chSTAU1 or shchMDA5 alone (Fig. 5*C*, bar 12 *vs.* bars 4 and 10); this outcomes suggests that chSTAU1 repression of chIFN-β promoter activity responsive to IBDV dsRNA stimulation is dependent on the chMDA5-mediated chIFN-β production pathway. These data show that chSTAU1 functions as a chMDA5 competitor in the binding of IBDV dsRNA to dampen the MDA5-mediated IFN-β induction.

STAU1 acts additively with VP3 to inhibit IBDV dsRNA–induced activation of IFN-β promoter

The viral capsid protein VP3, together with VP1, binds to IBDV dsRNA to assemble into RNP complexes (9, 10). We therefore also assessed the effect of chSTAU1–dsRNA interaction on the VP3 binding to the viral dsRNA by pull-down assays as in Fig. 5*A*. As expected, chSTAU1 and VP3 were pulled down by IBDV dsRNA (**Fig. 6*A***, lanes *2* and *1*, respectively). When the cell lysates containing both VP3 and chSTAU1 were used in the pull-down assay, both VP3 and chSTAU1 were pulled down by IBDV dsRNA concurrently (Fig. 6*A*, band δ′ and band γ′ in lane *3*). Although the level of VP3 binding to IBDV dsRNA was hardly affected by the presence of chSTAU1 (Fig. 6*A*, band δ′ in lane *3 vs.* band δ in lane *1*), the level of chSTAU1 binding to IBDV dsRNA was reduced by 60% in the presence of VP3 (Fig. 6*A*, band γ′ in lane *3 vs.* band γ in lane *2*; the histogram in the right panel). This finding suggests that the binding ability of VP3 for the viral dsRNA is stronger than that of chSTAU1, leading to VP3 outcompeting chSTAU1 binding to the viral dsRNA *in vitro*.

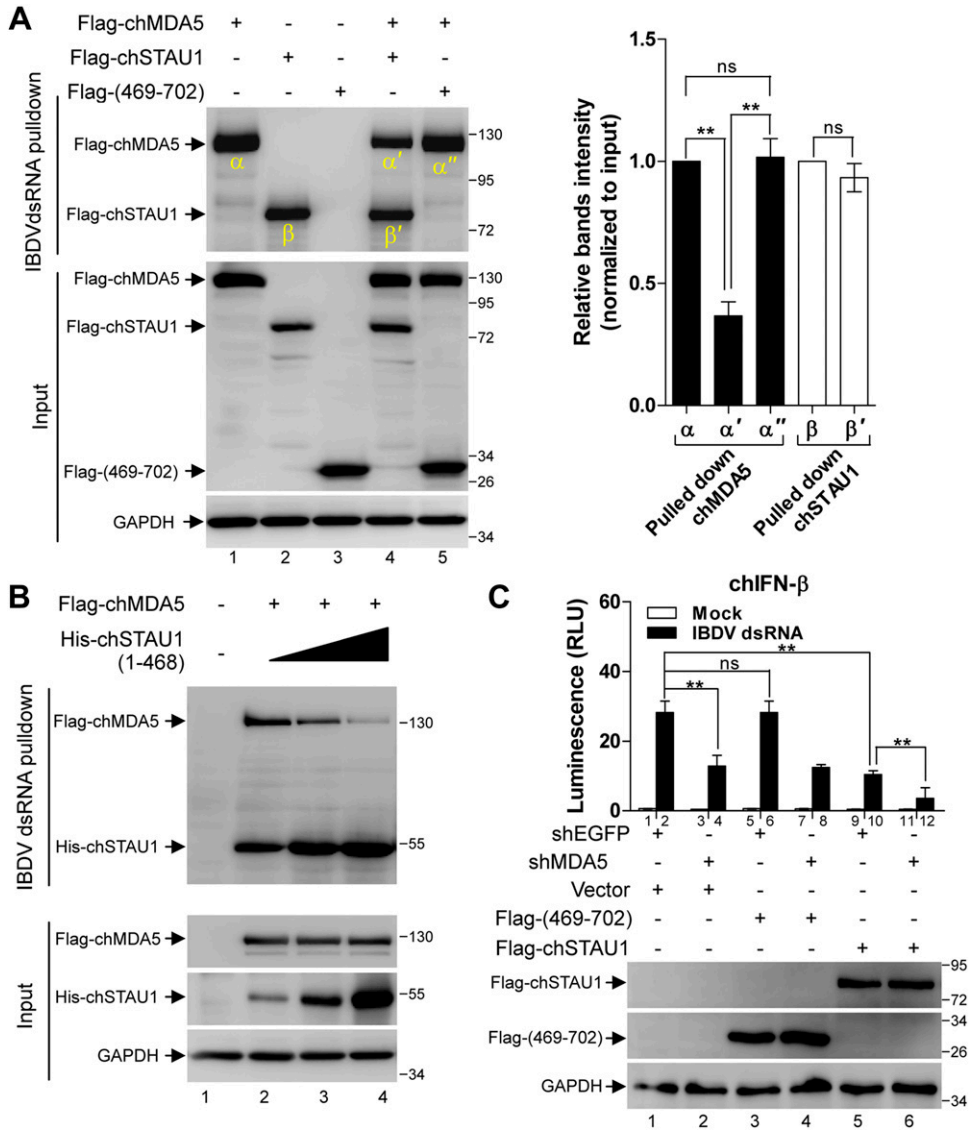

Figure 5. STAU1 competes with MDA5 for binding of IBDV dsRNA to counteract the IBDV dsRNA–induced activation of IFN-β promoter. *A*) chSTAU1 outcompetes chMDA5 binding to IBDV genomic dsRNA. HEK293T cells were transfected with the indicated plasmids for 36 h, and the whole cell lysates were extracted and subjected to the IBDV dsRNA pull-down assay. The Flag-chMDA5 or/and Flag-chSTAU1 present in the pull-down precipitates (upper panel) or in inputs (1:50) (lower panel) were detected by Western blot using the anti-Flag antibody. Histogram shows the relative intensity (normalized to the input) of chMDA5 (α, α′, and α″ bands) or chSTAU1 (β and β′ bands) presented in the viral dsRNA pulldown, which were quantified by using Quantity One software from 3 independent experiments (right panel). *B*) In a competition assay, chSTAU1 and chMDA5 compete for binding to IBDV dsRNA. Monolayer of HEK293T cells in 5 cm dishes were mock-transfected or transfected with Flag-chMDA5 (8 μg/dish). At 36 hpi, the whole cell lysate was extracted and incubated with increasing amounts of recombinant His-chSTAU1/(1–468) from 1 to 9 μg, followed by an IBDV dsRNA pull-down assay as described for *A*. The pulled down proteins were afterward analyzed by Western blot analysis using antibodies against Flag and His. *C*) The action of chMDA5 in promotion of IBDV dsRNA–induced activation of chIFN-β promoter was counteracted by overexpression of chSTAU1. Reporter assay was performed by cotransfection of the vector control or Flag-chSTAU1 together with luciferase report plasmids pGL3–chIFN-β and pRL-TK into DF-1 cells with stable expression of shchMDA5 or control shEGFP. The overexpressed chSTAU1 levels in cell lysates were monitored by Western blot analysis with an anti-Flag antibody, and the anti-GADPH blot was used as a loading control (lower panel). All the histograms were plotted based on the results of at least 3 independent experiments. Values are expressed as means ± SD. Ns, not significant. $^{**}P < 0.01$.

We next further determined the mutual effect between chSTAU1 and VP3 in the regulation of chIFN-β induction responsive to IBDV dsRNA stimulation. Transfection of DF-1 cells with either VP3 or chSTAU1 led to a suppression of the IFN-β promoter activity in response to the IBDV dsRNA stimulation (Fig. 6*B*, bars 8 and 6 *vs.* bar 2). Interestingly, cotransfection of VP3 and chSTAU1 in the presence of IBDV dsRNA stimulation resulted in an additional inhibition (>40%) on chIFN-β promoter activity compared with transfection of VP3 or chSTAU1 separately (Fig. 6*B*, bar 12 *vs.* bars 6 and 8). This phenomenon was not observed with the dsRNA-binding deficient mutant chSTAU1/(469–702) (Fig. 6*B*, bar 10). These data suggest that chSTAU1 and VP3 could act additively in the suppression of IBDV dsRNA–induced IFN-β production, which is IBDV dsRNA binding dependent. Furthermore, transient transfection of VP3 resulted in ~2-fold less inhibition of the IBDV dsRNA–induced activation of the IFN-β promoter in chSTAU1 knockdown cells than in the nontargeting control shEGFP cells (Fig. 6*C*, bar 8 *vs.* bar 6). This scenario indicates that the VP3-mediated inhibition of IFN-β induction is indeed at least partially contributed by cooperation with chSTAU1, and VP3 could not compensate for the deficiency of STAU1 in inhibiting IFN-β induction. Together, these data show that host chSTAU1 and VP3 act additively to down-regulate the viral dsRNA-mediated induction of IFN-β.

DISCUSSION

Many viruses can exploit host cell factors to contribute to their cellular entry, survival inside the host cell, replication, and evasion of host immune barriers. IBDV is known to

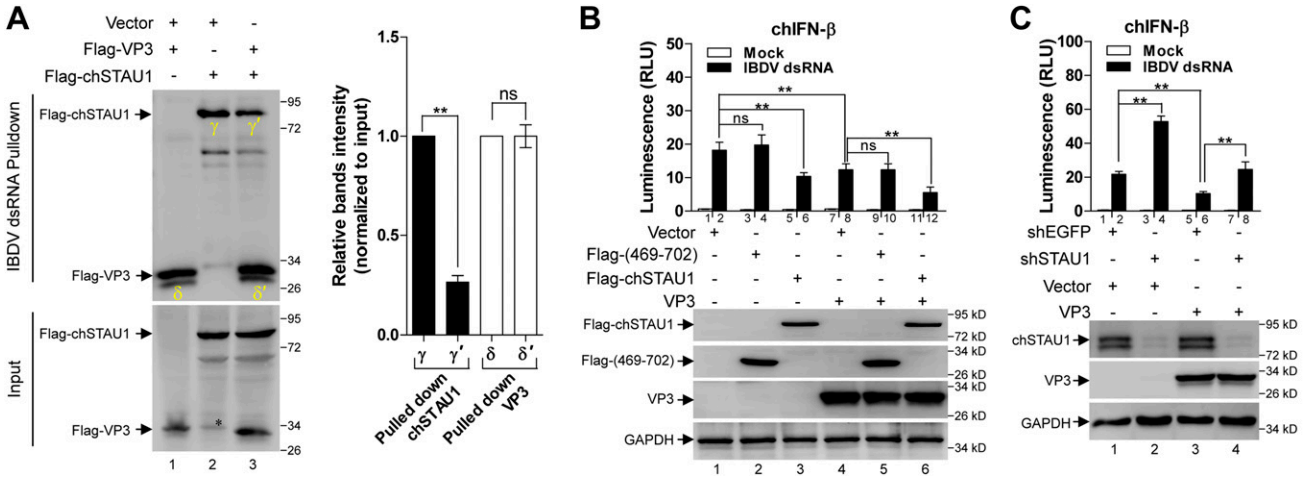

Figure 6. STAU1 acts additively with VP3 to repress viral dsRNA-mediated activation of IFN-β promoter. *A*) The level of VP3 binding to IBDV genomic dsRNA was not affected by the presence of chSTAU1. HEK293T cells were transfected with the indicated plasmids for 36 h, and the whole cell lysates were extracted for the IBDV dsRNA pulldown assay. The pulled-down Flag-chSTAU1 and/or Flag-VP3 proteins (left, upper panel) or inputs (left, lower panel) were analyzed by Western blot with anti-Flag antibody. Histogram shows the relative intensity (normalized to the input) of chSTAU1 (γ and γ′ bands) or VP3 (δ and δ′ bands) presented in the IBDV dsRNA pulldown, which was based on the quantified results of 3 independent experiments (right panel). *B*) chSTAU1 acts additively with VP3 to inhibit IBDV dsRNA–induced IFN-β production, which was monitored by luciferase reporter assay in DF-1 cells cotransfected with vector control, VP3, Flag-chSTAU1, or Flag-chSTAU1/(469–702) alone or in different combinations, as indicated, together with luciferase reporter with or without the intracellular stimulation of IBDV genomic dsRNA (upper panel). The level of protein expression was monitored by Western blot analysis with anti-Flag and anti-VP3. GAPDH was probed with anti-GAPDH as a loading control. *C*) Knockdown of chSTAU1 partially released the inhibitory effect of VP3 on IBDV dsRNA–induced activation of IFN-β promoter. Reporter assay was performed by cotransfection of the vector control or VP3 together with luciferase report plasmids pGL3–chIFN-β and pRL-TK in DF-1 cells with stable expression of shchSTAU1 or control shEGFP with or without the intracellular stimulation of IBDV genomic dsRNA. The overexpressed VP3 proteins and the shRNA silencing effect on STAU1 expression in cell lysates were monitored by Western blot analysis with anti-STAU1 and anti-VP3 antibodies, and the membrane was stripped and reprobed for GADPH as a loading control (lower panel). All the histograms were plotted based on the results of 3 independent experiments. Values are expressed as means ± SD. Ns, not significant. $^{**}P < 0.01$.

induce low levels of IFN expression in cell culture, and very virulent IBDV infection produces high levels of IFN (21), suggesting that a certain cellular mechanism operating in IBDV infection is responsible for preventing IFN induction. STAU1, a member of host cellular RNA binding proteins, plays an essential role in regulation of RNA transportation (50). In this study, we for the first time report that IBDV genomic dsRNA directly binds to host cellular STAU1 *via* its N-terminal moiety (residues 1–468), resulting in an enhancement of IBDV replication. The IBDV dsRNA–STAU1 interaction competes with the association of chMDA5 with IBDV dsRNA, which dampens the IBDV dsRNA–induced and MDA5-mediated IFN-β transcription. These findings thus provide a cellular mechanism for IBDV circumventing the host IFN antiviral responses.

The viral survival and replication inside the cells and induction of the innate antiviral response are crucial to determine the outcome of infection. The cytoplasmic pathogen recognition receptor chMDA5 detects IBDV infections and recognizes the viral dsRNA to initiate a chIFN-β antiviral response (20, 23). We found that chSTAU1 and chMDA5 compete for the binding to IBDV dsRNA as the binding of chSTAU1 to IBDV dsRNA resulted in a decrease in the association of chMDA5 but not VP3 with the viral dsRNA; this outcome suggests that chSTAU1- and chMDA5-binding sites are partially overlapped within the IBDV dsRNA, and that chMDA5 has less of a binding activity for viral dsRNA than chSTAU1. In contrast, the chSTAU1–dsRNA interaction had little effect on the binding of VP3 to the dsRNA; instead, the binding of chSTAU1 to the viral dsRNA was reduced in the presence of VP3 (Fig. 6*A*). This scenario argues that VP3, conversely, has stronger binding with IBDV dsRNA than chSTAU1, and is, therefore, much less inclined to release it once it is bound, which allows VP3 to displace STAU1 and associate dsRNA more easily for the initiation of viral dsRNA transcription and viral replication. These results therefore shed light on the relationship between VP3, chMDA5, and chSTAU1 in terms of their different binding ability for IBDV dsRNA and viral replication. Importantly, despite chSTAU1's weaker binding with IBDV dsRNA relative to VP3, there is a functional cooperation between VP3 and STAU1 in the down-regulation of IBDV dsRNA–induced activation of chIFN-β transcription (Fig. 6*B*): maximal inhibition of chIFN-β promoter activity was observed in the presence of chSTAU1 and VP3. Significantly, the ability of chSTAU1 to act additively with VP3 in down-regulation of IBDV dsRNA–induced IFN-β transcription is critically dependent on its viral dsRNA-binding capacity, indicating that chSTAU1 is a *bona fide* coactivator for VP3 in suppression of IBDV dsRNA–induced chIFN-β transcription. Thus, we propose that chSTAU1 suppresses the chIFN-β

antiviral response to promote IBDV proliferation *via* 2 routes: *1*) chSTAU1 competes with chMDA5 in binding IBDV dsRNA, which is chMDA5-dependent (Fig. 5); and *2*) chSTAU1 acts additively with VP3 in the down-regulation of the IBDV infection–induced IFN-β promoter activity (Fig. 6). Moreover, overexpression of wild-type chSTAU1 increased IBDV proliferation (Fig. 3) and led to the suppression of IBDV dsRNA–induced chIFN-β promoter activity (Fig. 4). These results were not observed in DF-1 cells transfected with dsRNA-binding deficient chSTAU1 mutants, suggesting that chSTAU1 inhibits IBDV dsRNA–mediated chIFN-β induction to promote IBDV productive infection, which is dependent on chSTAU1–dsRNA binding.

There is increasing evidence that chSTAU1 plays crucial roles in multiple steps in the life cycle and stimulates productive infection of many RNA viruses, including HIV, influenza A virus, and HCV (34, 51, 52). However, the working mechanism is different. STAU1 stimulates HCV replication by interacting with multiple components of HCV, including 3′ and 5′ nontranslated regions of the HCV genome, and viral nonstructural proteins of NS5B and NS3 (52). STAU1 interacts with the structural proteins Gag of HIV (53), and with viral RNPs and NS1 of influenza virus (33), to promote the replication of HIV and influenza virus, respectively.

We observed that the IBDV proliferation in chSTAU1 knockdown cells decreased at a late stage of 12 hpi, a much lower rate than did replication in the control cells (Fig. 2). However, the replication at 6 hpi, an early stage of infection when the virus has completed cellular entry, between the chSTAU1 knockdown cells and the control cells did not differ significantly. Thus, although the early step of cellular entry of IBDV was scarcely affected, IBDV replication after the viral cellular entry was suppressed upon the down-regulation of cellular chSTAU1.

Knockdown of chMDA5 and overexpression of chSTAU1 lead to a significant inhibition of chIFN-β promoter activity when applied separately, and interestingly, in combination give rise to even greater inhibition (Fig. 5C). Furthermore, most of the inhibitory effect of chSTAU1 on chIFN-β promoter activity was retained in chMDA5-deficient cells. These data suggest that the chSTAU1-mediated chIFN-β suppression is, at least partially, chMDA5 independent, namely that there exists an additional chMDA5-independent mechanism that contributes to the inhibitory effect of chSTAU1 on the IFN-β transcription. Many RNA virus infection triggers activation of PKR-eIF2α pathway by specific phosphorylation, and PKR serves as an essential cytoplasmic PRR for viral dsRNA and mediates IFN antiviral activities of virus-infected cells (54). Knockdown of STAU1 led to an increase in the activation of the PKR-eIF2α signaling pathway during IBDV infection (Fig. 4*G* and Supplemental Fig. 2B), suggesting that the phosphorylation status of the PKR-eIF2α module could be modulated by STAU1 upon IBDV infection, which could contribute to the inhibitory effect of chSTAU1 on IFN-β induction. One explanation for this phenomenon could be that down-regulation of STAU1 frees up more viral dsRNA that activates the cellular dsRNA sensor PKR, leading to phosphorylation of eIF2α (**Fig. 7**). Despite an attenuation of cellular mRNA translation, phosphorylation of eIF2α concomitantly assists in the production of IFN and subsequently restricts virus replication (55–57).

Compared with chMDA5, the interaction of VP3 with IBDV dsRNA was not affected in the presence of chSTAU1, correlating with the observation that chSTAU1 and VP3 have an addictive effect in the down-regulation of the IBDV dsRNA–induced chIFN-β promoter activity and chIFN-β gene transcription (Fig. 6). The exact mechanism for how chSTAU1 works together with VP3 to promote IBDV replication and to suppress the IBDV dsRNA–induced chIFN-β production are not understood; however, it is likely that chSTAU1 may suppress chIFN-β induction by functioning as a primary mRNA regulator in addition to its role as a suppressor of chIFN-β induction *via* competition with chMDA5 for IBDV dsRNA

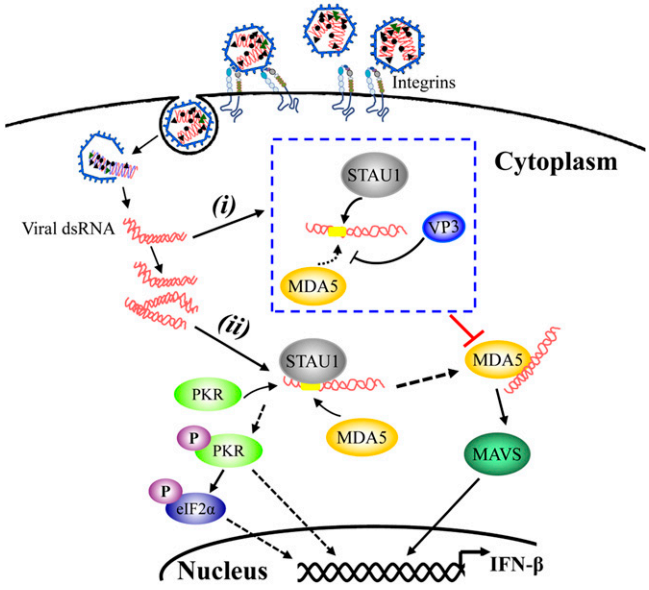

Figure 7. Proposed model for competition between STAU1 and MDA5 for IBDV dsRNA binding in the regulation of β-IFN during IBDV infection. In this model, we proposed that chSTAU1 subverts IBDV-induced production of IFN-β *via* competition with chMDA5 for the viral dsRNA binding, which is depicted as follows. *i*) At the early stage of IBDV infection, the viral dsRNA released in the cytoplasm is of a small amount, and is preferentially bound by VP3 together with chSTAU1 because IBDV dsRNA binds stronger to VP3 and STAU1 than to MDA5 (Fig. 5A). These associations preclude access of chMDA5 to the viral dsRNA, preventing MDA5-dependent and the viral dsRNA-mediated induction of chIFN-β and thus promoting virus proliferation. *ii*) When the viral dsRNA is accumulated to high levels at the late stage of infection, in return, MDA5 is able to compete with chSTAU1 and/or VP3 that has been bound to the IBDV dsRNA to associate the viral dsRNA, resulting in an increase in chIFN-β production. Alternatively, PKR-eIF2α signaling axis can be activated with the increase of free viral dsRNA, which assists in the production of antiviral IFN (55–57). STAU1–dsRNA binding could also pose a negative effect on the activation of PKR-eIF2α signaling axis, leading to an inhibition on IFN-β induction. Thus, the temporal competition between STAU1 and MDA5 and/or PKR for IBDV dsRNA binding determines the increase or decrease in the IFN-β production at different stages of the viral infection.

binding. VP3, together with VP1, binds dsRNA to form the RNP complexes, which play a key role in the IBDV replication (12, 58). Thus, the chSTAU1–dsRNA interaction may specifically aid VP3-containing RNP complexes in trafficking to viral replication sites to promote IBDV replication and to modulate the chIFN-β dynamics during the viral infection. The precise role of chSTAU1 involved in the functions of the VP3-containing RNP complexes in the IBDV dsRNA transcription and initiation of viral protein translation awaits future investigation.

In summary, based on the results of the current study, we propose a model explaining how IBDV dsRNA interacts with host factor chSTAU1 to suppress the IFN antiviral activities of the virus-infected cells, resulting in an enhancement of the viral productive infection. The antagonism of IFN induction by IBDV occurs through host STAU1 together with VP3-mediated sequestering the viral dsRNA from MDA5, thereby preventing viral dsRNA–mediated IFN-β induction (Fig. 7). These findings provide new insights into the strategies used by IBDV to evade host IFN antiviral response. FJ

ACKNOWLEDGMENTS

This work was supported by the Natural Scientific Foundation of Zhejiang Province (LY18C180002), the China Postdoctoral Science Foundation (2017M621977), the National Natural Science Foundation of China (31470840 and 31502061), the Science and Technology Foundation of Jiangsu province (BK20131181), and the ZAFU Research and Development Fund (2014FR019 and 2015FR008). The authors declare no conflicts of interest.

AUTHOR CONTRIBUTIONS

H. Liu conceived the study; C. Ye and H. Liu designed the research; C. Ye, Z. Yu, Y. Xiong, Y. Wang, Y. Ruan, Y. Guo, M. Chen, S. Luan, and E. Zhang performed research; C. Ye, Z. Yu, Y. Xiong, and H. Liu analyzed data; Y. Xiong contributed new analytic tools; H. Liu and C. Ye wrote the paper; Y. Xiong and H. Liu revised the paper; and H. Liu finalized the paper.

REFERENCES

1. Sharma, J. M., Kim, I.-J., Rautenschlein, S., and Yeh, H.-Y. (2000) Infectious bursal disease virus of chickens: pathogenesis and immunosuppression. *Dev. Comp. Immunol.* **24**, 223–235
2. Von Einem, U. I., Gorbalenya, A. E., Schirrmeier, H., Behrens, S. E., Letzel, T., and Mundt, E. (2004) VP1 of infectious bursal disease virus is an RNA-dependent RNA polymerase. *J. Gen. Virol.* **85**, 2221–2229
3. Lombardo, E., Maraver, A., Espinosa, I., Fernández-Arias, A., and Rodriguez, J. F. (2000) VP5, the nonstructural polypeptide of infectious bursal disease virus, accumulates within the host plasma membrane and induces cell lysis. *Virology* **277**, 345–357
4. Méndez, F., de Garay, T., Rodríguez, D., and Rodríguez, J. F. (2015) Infectious bursal disease virus VP5 polypeptide: a phosphoinositide-binding protein required for efficient cell-to-cell virus dissemination. *PLoS One* **10**, e0123470
5. Spies, U., Müller, H., and Becht, H. (1989) Nucleotide sequence of infectious bursal disease virus genome segment A delineates two major open reading frames. *Nucleic Acids Res.* **17**, 7982
6. Kibenge, F. S., Jackwood, D. J., and Mercado, C. C. (1990) Nucleotide sequence analysis of genome segment A of infectious bursal disease virus. *J. Gen. Virol.* **71**, 569–577
7. Lee, C. C., Ko, T. P., Chou, C. C., Yoshimura, M., Doong, S. R., Wang, M. Y., and Wang, A. H.. (2006) Crystal structure of infectious bursal disease virus VP2 subviral particle at 2.6A resolution: implications in virion assembly and immunogenicity. *J. Struct. Biol.* **155**, 74–86
8. Oña, A., Luque, D., Abaitua, F., Maraver, A., Castón, J. R., and Rodríguez, J. F. (2004) The C-terminal domain of the pVP2 precursor is essential for the interaction between VP2 and VP3, the capsid polypeptides of infectious bursal disease virus. *Virology* **322**, 135–142
9. Tacken, M. G., Peeters, B. P., Thomas, A. A., Rottier, P. J., and Boot, H. J. (2002) Infectious bursal disease virus capsid protein VP3 interacts both with VP1, the RNA-dependent RNA polymerase, and with viral double-stranded RNA. *J. Virol.* **76**, 11301–11311
10. Lombardo, E., Maraver, A., Castón, J. R., Rivera, J., Fernández-Arias, A., Serrano, A., Carrascosa, J. L., and Rodriguez, J. F. (1999) VP1, the putative RNA-dependent RNA polymerase of infectious bursal disease virus, forms complexes with the capsid protein VP3, leading to efficient encapsidation into virus-like particles. *J. Virol.* **73**, 6973–6983
11. Ferrero, D., Garriga, D., Navarro, A., Rodríguez, J. F., and Verdaguer, N. (2015) Infectious bursal disease virus VP3 upregulates VP1-mediated RNA-dependent RNA replication. *J. Virol.* **89**, 11165–11168
12. Ye, C., Wang, Y., Zhang, E., Han, X., Yu, Z., and Liu, H. (2018) VP1 and VP3 are required and sufficient for translation initiation of uncapped infectious bursal disease virus genomic double-stranded RNA. *J. Virol.* **92**, e01345–e17
13. Le Bon, A., and Tough, D. F. (2002) Links between innate and adaptive immunity via type I interferon. *Curr. Opin. Immunol.* **14**, 432–436
14. Kato, H., Takahasi, K., and Fujita, T. (2011) RIG-I-like receptors: cytoplasmic sensors for non-self RNA. *Immunol. Rev.* **243**, 91–98
15. Kato, H., Takeuchi, O., Sato, S., Yoneyama, M., Yamamoto, M., Matsui, K., Uematsu, S., Jung, A., Kawai, T., Ishii, K. J., Yamaguchi, O., Otsu, K., Tsujimura, T., Koh, C. S., Reis e Sousa, C., Matsuura, Y., Fujita, T., and Akira, S. (2006) Differential roles of MDA5 and RIG-I helicases in the recognition of RNA viruses. *Nature* **441**, 101–105
16. Loo, Y. M., Fornek, J., Crochet, N., Bajwa, G., Perwitasari, O., Martinez-Sobrido, L., Akira, S., Gill, M. A., García-Sastre, A., Katze, M. G., and Gale, M., Jr. (2008) Distinct RIG-I and MDA5 signaling by RNA viruses in innate immunity. *J. Virol.* **82**, 335–345
17. Kawai, T., Takahashi, K., Sato, S., Coban, C., Kumar, H., Kato, H., Ishii, K. J., Takeuchi, O., and Akira, S. (2005) IPS-1, an adaptor triggering RIG-I- and Mda5-mediated type I interferon induction. *Nat. Immunol.* **6**, 981–988
18. Barber, M. R., Aldridge, J. R., Jr., Webster, R. G., and Magor, K. E. (2010) Association of RIG-I with innate immunity of ducks to influenza [published erratum appears in Proc. Natl. Acad. Sci. USA (2013), 110, 7958]. *Proc. Natl. Acad. Sci. USA* **107**, 5913–5918
19. Hayashi, T., Watanabe, C., Suzuki, Y., Tanikawa, T., Uchida, Y., and Saito, T. (2014) Chicken MDA5 senses short double-stranded RNA with implications for antiviral response against avian influenza viruses in chicken. *J. Innate Immun.* **6**, 58–71
20. Karpala, A. J., Stewart, C., McKay, J., Lowenthal, J. W., and Bean, A. G. (2011) Characterization of chicken Mda5 activity: regulation of IFN-β in the absence of RIG-I functionality. *J. Immunol.* **186**, 5397–5405
21. Eldaghayes, I., Rothwell, L., Williams, A., Withers, D., Balu, S., Davison, F., and Kaiser, P. (2006) Infectious bursal disease virus: strains that differ in virulence differentially modulate the innate immune response to infection in the chicken bursa. *Viral Immunol.* **19**, 83–91
22. Li, Z., Wang, Y., Li, X., Li, X., Cao, H., and Zheng, S. J. (2013) Critical roles of glucocorticoid-induced leucine zipper in infectious bursal disease virus (IBDV)-induced suppression of type I Interferon expression and enhancement of IBDV growth in host cells via interaction with VP4. *J. Virol.* **87**, 1221–1231
23. Ye, C., Jia, L., Sun, Y., Hu, B., Wang, L., Lu, X., and Zhou, J. (2014) Inhibition of antiviral innate immunity by birnavirus VP3 protein via blockage of viral double-stranded RNA binding to the host cytoplasmic RNA detector MDA5. *J. Virol.* **88**, 11154–11165
24. Saelens, X., Kalai, M., and Vandenabeele, P. (2001) Translation inhibition in apoptosis: caspase-dependent PKR activation and eIF2-α phosphorylation. *J. Biol. Chem.* **276**, 41620–41628
25. McAllister, C. S., Taghavi, N., and Samuel, C. E. (2012) Protein kinase PKR amplification of interferon β induction occurs through initiation factor eIF-2α-mediated translational control. *J. Biol. Chem.* **287**, 36384–36392
26. Busnadiego, I., Maestre, A. M., Rodríguez, D., and Rodríguez, J. F. (2012) The infectious bursal disease virus RNA-binding VP3 polypeptide inhibits PKR-mediated apoptosis. *PLoS One* **7**, e46768

27. Cubas-Gaona, L. L., Diaz-Beneitez, E., Ciscar, M., Rodríguez, J. F., and Rodríguez, D. (2018) Exacerbated apoptosis of cells infected with infectious bursal disease virus upon exposure to interferon alpha. *J. Virol.* **92**
28. Kim, M. Y., Park, J., Lee, J. J., Ha, D. H., Kim, J., Kim, C. G., Hwang, J., and Kim, C. G. (2014) Staufen1-mediated mRNA decay induces requiem mRNA decay through binding of Staufen1 to the requiem 3'UTR. *Nucleic Acids Res.* **42**, 6999–7011
29. Furic, L., Maher-Laporte, M., and DesGroseillers, L. (2008) A genome-wide approach identifies distinct but overlapping subsets of cellular mRNAs associated with Staufen1- and Staufen2-containing ribonucleoprotein complexes. *RNA* **14**, 324–335
30. Mouland, A. J., Mercier, J., Luo, M., Bernier, L., DesGroseillers, L., and Cohen, É. A. (2000) The double-stranded RNA-binding protein Staufen is incorporated in human immunodeficiency virus type 1: evidence for a role in genomic RNA encapsidation. *J. Virol.* **74**, 5441–5451
31. Milev, M. P., Brown, C. M., and Mouland, A. J. (2010) Live cell visualization of the interactions between HIV-1 Gag and the cellular RNA-binding protein Staufen1. *Retrovirology* **7**, 41
32. Blackham, S. L., and McGarvey, M. J. (2013) A host cell RNA-binding protein, Staufen1, has a role in hepatitis C virus replication before virus assembly. *J. Gen. Virol.* **94**, 2429–2436
33. Lee, J. H., Oh, J. Y., Pascua, P. N. Q., Kim, E. G., Choi, Y. K., and Kim, H. K. (2011) Impairment of the Staufen1-NS1 interaction reduces influenza viral replication. *Biochem. Biophys. Res. Commun.* **414**, 153–158
34. De Lucas, S., Peredo, J., Marión, R. M., Sánchez, C., and Ortín, J. (2010) Human Staufen1 protein interacts with influenza virus ribonucleoproteins and is required for efficient virus multiplication. *J. Virol.* **84**, 7603–7612
35. Thomas, M. G., Martinez Tosar, L. J., Desbats, M. A., Leishman, C. C., and Boccaccio, G. L. (2009) Mammalian Staufen 1 is recruited to stress granules and impairs their assembly. *J. Cell Sci.* **122**, 563–573
36. Yu, L., Li, J. R., Huang, Y. W., Dikki, J., and Deng, R. (2001) Molecular characteristics of full-length genomic segment A of three infectious bursal disease viruses in China: two attenuated strains and one virulent field strain. *Avian Dis.* **45**, 862–874
37. Ye, C., Han, X., Yu, Z., Zhang, E., Wang, L., and Liu, H. (2017) Infectious bursal disease virus activates c-Src to promote α4β1 integrin-dependent viral entry by modulating the downstream Akt-RhoA GTPase-actin rearrangement cascade. *J. Virol.* **91**
38. Peritz, T., Zeng, F., Kannanayakal, T. J., Kilk, K., Eiríksdóttir, E., Langel, U., and Eberwine, J. (2006) Immunoprecipitation of mRNA-protein complexes. *Nat. Protoc.* **1**, 577–580
39. Chatel-Chaix, L., Clément, J. F., Martel, C., Bériault, V., Gatignol, A., DesGroseillers, L., and Mouland, A. J. (2004) Identification of Staufen in the human immunodeficiency virus type 1 Gag ribonucleoprotein complex and a role in generating infectious viral particles. *Mol. Cell. Biol.* **24**, 2637–2648
40. Boot, H. J., ter Huurne, A. H., and Peeters, B. P. (2000) Generation of full-length cDNA of the two genomic dsRNA segments of infectious bursal disease virus. *J. Virol. Methods* **84**, 49–58
41. Li, Y., Chen, R., Zhou, Q., Xu, Z., Li, C., Wang, S., Mao, A., Zhang, X., He, W., and Shu, H. B. (2012) LSm14A is a processing body-associated sensor of viral nucleic acids that initiates cellular antiviral response in the early phase of viral infection. *Proc. Natl. Acad. Sci. USA* **109**, 11770–11775
42. French, A. P., Mills, S., Swarup, R., Bennett, M. J., and Pridmore, T. P. (2008) Colocalization of fluorescent markers in confocal microscope images of plant cells. *Nat. Protoc.* **3**, 619–628
43. Kim, Y. K., Furic, L., Parisien, M., Major, F., DesGroseillers, L., and Maquat, L. E. (2007) Staufen1 regulates diverse classes of mammalian transcripts. *EMBO J.* **26**, 2670–2681
44. Vessey, J. P., Macchi, P., Stein, J. M., Mikl, M., Hawker, K. N., Vogelsang, P., Wieczorek, K., Vendra, G., Riefler, J., Tübing, F., Aparicio, S. A., Abel, T., and Kiebler, M. A. (2008) A loss of function allele for murine Staufen1 leads to impairment of dendritic Staufen1-RNP delivery and dendritic spine morphogenesis. *Proc. Natl. Acad. Sci. USA* **105**, 16374–16379
45. Anderson, P., and Kedersha, N. (2008) Stress granules: the Tao of RNA triage. *Trends Biochem. Sci.* **33**, 141–150
46. Thomas, M. G., Martinez Tosar, L. J., Loschi, M., Pasquini, J. M., Correale, J., Kindler, S., and Boccaccio, G. L. (2005) Staufen recruitment into stress granules does not affect early mRNA transport in oligodendrocytes. *Mol. Biol. Cell* **16**, 405–420
47. García-Sastre, A., and Biron, C. A. (2006) Type 1 interferons and the virus-host relationship: a lesson in détente. *Science* **312**, 879–882
48. Lee, C. C., Wu, C. C., and Lin, T. L. (2014) Chicken melanoma differentiation-associated gene 5 (MDA5) recognizes infectious bursal disease virus infection and triggers MDA5-related innate immunity. *Arch. Virol.* **159**, 1671–1686
49. Smith, G. L. (1994) Virus strategies for evasion of the host response to infection. *Trends Microbiol.* **2**, 81–88
50. Sossin, W. S., and DesGroseillers, L. (2006) Intracellular trafficking of RNA in neurons. *Traffic* **7**, 1581–1589
51. Abrahamyan, L. G., Chatel-Chaix, L., Ajamian, L., Milev, M. P., Monette, A., Clément, J. F., Song, R., Lehmann, M., DesGroseillers, L., Laughrea, M., Boccaccio, G., and Mouland, A. J. (2010) Novel Staufen1 ribonucleoproteins prevent formation of stress granules but favour encapsidation of HIV-1 genomic RNA. *J. Cell Sci.* **123**, 369–383
52. Dixit, U., Pandey, A. K., Mishra, P., Sengupta, A., and Pandey, V. N. (2016) Staufen1 promotes HCV replication by inhibiting protein kinase R and transporting viral RNA to the site of translation and replication in the cells. *Nucleic Acids Res.* **44**, 5271–5287
53. Chatel-Chaix, L., Abrahamyan, L., Fréchina, C., Mouland, A. J., and DesGroseillers, L. (2007) The host protein Staufen1 participates in human immunodeficiency virus type 1 assembly in live cells by influencing pr55Gag multimerization. *J. Virol.* **81**, 6216–6230
54. Langland, J. O., Cameron, J. M., Heck, M. C., Jancovich, J. K., and Jacobs, B. L. (2006) Inhibition of PKR by RNA and DNA viruses. *Virus Res.* **119**, 100–110
55. Balachandran, S., Roberts, P. C., Brown, L. E., Truong, H., Pattnaik, A. K., Archer, D. R., and Barber, G. N. (2000) Essential role for the dsRNA-dependent protein kinase PKR in innate immunity to viral infection. *Immunity* **13**, 129–141
56. Cláudio, N., Dalet, A., Gatti, E., and Pierre, P. (2013) Mapping the crossroads of immune activation and cellular stress response pathways. *EMBO J.* **32**, 1214–1224
57. Schröder, M., and Kaufman, R. J. (2005) The mammalian unfolded protein response. *Annu. Rev. Biochem.* **74**, 739–789
58. Luque, D., Saugar, I., Rejas, M. T., Carrascosa, J. L., Rodríguez, J. F., and Castón, J. R. (2009) Infectious Bursal disease virus: ribonucleoprotein complexes of a double-stranded RNA virus. *J. Mol. Biol.* **386**, 891–901

Received for publication January 30, 2018.
Accepted for publication June 18, 2018.